Aus dem Institut für Virologie

des Fachbereichs Veterinärmedizin

der Freien Universität Berlin

Role of the Marek's disease virus (MDV) interleukin-8 (vIL-8) in lymphoma formation and recruitment of target cells

Inaugural-Dissertation

zur Erlangung des Grades eines

Doktors der Veterinärmedizin

an der

Freien Universität Berlin

vorgelegt von

Annemarie Theresia Engel geb. Egerer

Tierärztin

aus Wuppertal

Berlin 2012

Journal-Nr.: 3602

Gedruckt mit Genehmigung des Fachbereichs Veterinärmedizin
der Freien Universität Berlin

Dekan:	Univ.-Prof. Dr. Jürgen Zentek
Erster Gutachter:	Univ.-Prof. Dr. Nikolaus Osterrieder
Zweiter Gutachter:	Univ.-Prof. Dr. Hafez Mohamed Hafez
Dritter Gutachter:	Univ.-Prof. Dr. Susanne Hartmann

Deskriptoren (nach CAB-Thesaurus):
Marek's disease virus, chemotaxis, chemokines, B cells, T cells, pathogenesis, pathogenesisrelated proteins, bacterial artificial chromosomes, chickens, binding, ligands, receptors, animal experiments, tumors

Tag der Promotion: 10.05.2013

Bibliografische Information der *Deutschen Nationalbibliothek*
Die Deutsche Nationalbibliothek verzeichnet diese Publikation in der Deutschen Nationalbibliografie; detaillierte bibliografische Daten sind im Internet über <http://dnb.ddb.de> abrufbar.

ISBN: 978-3-86387-320-2
Zugl.: Berlin, Freie Univ., Diss., 2012
Dissertation, Freie Universität Berlin
D 188

Choriner Str. 85 - 10119 Berlin
verlag@menschundbuch.de – www.menschundbuch.de

Role of the Marek's disease virus (MDV) interleukin-8 (vIL-8) in lymphoma formation and recruitment of target cells

Summary

Marek's disease virus (MDV) is a cell-associated and highly oncogenic alpha-herpesvirus that infects chickens. The MDV genome consists of a unique long (U_L) and a unique short region (U_S), each flanked by inverted repeat regions (R_L, R_S). In the R_L, a number of unique genes are located that are involved in MDV pathogenesis and tumorigenesis. To facilitate generation of recombinant viruses harboring mutations in the MDV R_L region, I deleted most of the internal repeat long (IR_L) in pRB-1B (vΔIR_L) leaving short sequence ends of the region intact to allow restoration of the sequence via homologous recombination during MDV replication. I used vΔIR_L as a tool to modify the viral interleukin-8 (vIL-8), a CXC chemokine expressed during both the lytic and latent stages of MDV infection to investigate its role in MDV pathogenesis. Previously, a virus with a deletion of the entire vIL-8 open reading frame (ORF) was shown to be severely impaired in disease progression and tumor development in infected chickens. Marek's disease (MD) and tumor incidence was reduced to 4-10% in chickens infected with vIL-8 deletion viruses compared to more than 90% upon infection with parental virus. However, it remained unclear whether this phenotype was caused by the lack of secreted vIL-8 or vIL-8 splice variants that fuse exons II and III of vIL-8 to several upstream open reading frames, including the viral oncoprotein Meq, RLORF4 and RLORF5a. To specifically examine the role of secreted vIL-8 in MDV pathogenesis, I constructed a recombinant virus in which the vIL-8 start codon located in exon I was mutated (vΔMetvIL-8). This mutant lacked expression of vIL-8 without affecting Meq-vIL-8 splice variants. Loss of secreted vIL-8 resulted in a highly reduced disease and tumor incidence in chickens infected with vΔMetvIL-8 by the intra-abdominal route. Although vΔMetvIL-8 was still able to spread to naïve animals via the natural route, infection and lymphomagenesis in contact animals was severely impaired. To determine the target cells of the vIL-8 chemokine, I generated purified recombinant vIL-8 and could demonstrate that it efficiently binds to and induces chemotaxis of B cells, the main target for lytic MDV replication. Furthermore, I could show that vIL-8 also interacts with $CD4^+CD25^+$ T cells, a putative target for MDV transformation. Our data provide evidence that vIL-8 attracts B cells and $CD4^+CD25^+$ T cells the targets for both lytic and latent infection.

Chemokines usually contain a number of conserved motifs that are important for chemokine function. vIL-8 contains a DKR motif at the N-terminus. In other CXC chemokines, the motif in this position is responsible for the specific binding of the chemokine

to its receptor on target cells. To address the role of the DKR motif in the binding specificity, I mutated the DKR motif to ELR which is present in the closely related chemokine interleukin-8 (IL-8). Mutating the DKR motif to ELR did not alter the binding properties of vIL-8 suggesting that DKR is not important for specificity of vIL-8 binding.

Previously, a role for C-terminal domains of CXC cytokines in angiogenesis during tumor formation has been suggested. To determine whether the vIL-8 C-terminus can influence tumor formation, I generated a C-terminal deletion mutant (vΔCT-vIL-8). *In vitro*, this virus replicated comparable to parental and revertant virus. *In vivo*, we only observed only a slight reduction in disease and tumor incidence in chickens infected with vΔCT-vIL-8, suggesting that the C-terminus plays a minor role in the tumorigenesis and pathogenesis and neither affects vIL-8 nor vIL-8 splice variant function.

Despite a plethora of studies addressing the establishment of MDV infection and pathogenesis, the exact mechanisms are still not well understood. To develop a tool that facilitates detection of and discrimination between lytic and latently infected cells *in vivo*, we generated a markervirus containing fluorescently labeled proteins indicating the state of the infection of the infected cells. For this purpose, we fused the red fluorescent protein (RFP) to the C-terminus of UL47, a protein expressed only during lytic replication, and the green fluorescent protein (GFP) to the C-terminus of Meq, a protein expressed during latency and in transformed cells (vUL47-RFP_Meq-GFP). *In vitro*, vUL47-RFP_Meq-GFP replicated comparable to parental virus and expression of the fluorescent proteins could be observed. Intriguingly, vUL47-RFP_Meq-GFP did not induce disease, suggesting that fusion of GFP to the C-terminus of Meq affects its function in transformation and tumorigenesis.

Die Rolle des Marek's disease Virus (MDV) interleukin-8 (vIL-8) bei der Lymphomentstehung und der Rekrutierung von Zielzellen.

Zusammenfassung

Das Marek's disease Virus ist ein zellassoziiertes, onkogenes Alphaherpesvirus, das Hühner infiziert. Das MDV-Genom besteht aus Genomabschnitten, die als unique long (U_L) und unique short regions (U_S) bezeichnet, und jeweils von invertierten, homologen repeats (R_L, R_S) eingerahmt werden. Innerhalb der R_L befinden sich diploide Gene, die spezifisch für MDV sind, und für die in vielen Studien eine wichtige Rolle in der Pathogenese und Tumorigenese der Marek'schen Krankheit gezeigt wurde. Um das Erstellen von rekombinanten Viren im Bereich der R_L zu vereinfachen, habe ich den Großteil des internal repeat long (IR_L) entfernt, wobei kurze Endsequenzen des IR_L im Virusgenom verblieben sind, die die Wiederherstellung der Sequenz durch homologe Rekombination während der Replikation ermöglichen. Dieses ΔIR_L Virus bildet die Grundlage, um die Rolle des viralen Interleukin-8 (vIL-8), einem CXC Chemokin, in der MDV Pathogenese zu untersuchen, das sowohl während der lytischen als auch der latenten Infektion in Zellen exprimiert wird. Bisherige Studien zeigten, dass nach Infektion mit einer vIL-8 Deletionsmutante, bei der der gesamte open reading frame (ORF) entfernt wurde, Tumor- und Marek's Disease Inzidenz nur noch bei 4-10% gegenüber mehr als 90% bei Hühnern, die mit dem hoch pathogenen, parentalen Virusstamm RB-1B infiziert wurden, lagen. Es blieb jedoch unklar, ob dieser Phänotyp des vIL-8 Deletionsvirus auf die fehlende vIL-8 Sekretion oder auf den Verlust von vIL-8 splice Varianten zurückzuführen ist, bei denen die Exons II und III von vIL-8 an einige andere Gene, wie etwa das virale Onkoprotein Meq, RLORF4, oder RLORF5a gespleißt werden. Um deshalb die Rolle des sekretierten vIL-8 für die Pathogenese zu untersuchen, habe ich ein rekombinantes Virus, vΔMetvIL-8, erstellt, bei dem das in Exon I enthaltene Startcodon mutiert ist. Dieser Mutante fehlt die vIL-8 Expression, lässt aber die Expression von vIL-8 Spleißvarianten unberührt. *In vivo* führte die fehlende vIL-8 Sekretion zu einer stark reduzierten Marek's Disease und Tumorinzidenz nach intra abdominaler Infektion. Obwohl vΔMetvIL-8 Viren noch auf naive Hühner auf dem natürlichen Infektionsweg übertragbar waren, verursachte das Virus jedoch keine Krankheitssymptome oder Lymphome in den Kontakttieren. In *in vitro* Assays mit aufgereinigtem, rekombinantem vIL-8 band effektiv an B Zellen, in denen MDV lytisch repliziert und induzierte Chemotaxis. Außerdem interagierte vIL-8 auch mit $CD4^+CD25^+$ T Zellen, die das Virus möglicherweise für die Transformation nutzt. Diese Daten sprechen daher dafür, dass vIL-8 B Zellen und

möglicherweise $CD4^+$ $CD25^+$ T Zellen mit aktiviertem Phänotyp und für die lytische und latent Infektion rekrutiert.

Chemokine besitzen eine Reihe an konservierten Motiven, die für die Chemokinfunktion von Bedeutung sind. vIL-8 hat ein DKR Motiv am N-Terminus, und es wurde für andere Chemokine gezeigt, dass das Aminosäuremotiv an dieser Stelle für das spezifische Binden des Chemokins an seinen Rezeptor verantwortlich ist. Um die Rolle des DKR Motivs für die Bindungsspezifität zu bestimmen, mutierte ich DKR zu ELR, das im nahe verwandten Interleukin-8 (IL-8) zu finden ist. Die Mutation zu ELR veränderte jedoch die Bindungseigenschaften von vIL-8 nicht, was darauf hinweist, dass DKR für die Bindungsspezifität keine Rolle spielt.

In früheren Studien wurde außerdem eine Rolle für die C-terminale Domäne von CXC Chemokinen für die Angiogenese während der Tumorentstehung vorgeschlagen. Um zu sehen, ob der C-terminus von vIL-8 möglicherweise einen ähnlichen Einfluss auf die Tumorentstehung hat, stellte ich eine C-terminale Deletionsmutante her (vΔCT-vIL-8). *In vitro* replizierte dieses Virus vergleichbar mit dem parentalen Virus. *In vivo* beobachtete ich jedoch nur eine geringfügige Reduktion an Erkrankungen und Tumoren, was darauf hindeutet, dass der C-terminus nur eine untergeordnete Rolle bei der Tumorigenese spielt und weder für vIL-8 noch für vIL-8 Spleißvarianten eine herausragende Bedeutung hat.

Trotz einer Vielzahl von Studien, die die Etablierung der MDV Infektion und Pathogenese Untersuchen, sind die genauen Mechanismen noch unzureichend verstanden. Um ein Hilfsmittel für die Detektion und Differenzierung von lytisch und latent infizierten Zellen zu entwickeln, erstellte ich ein rekombinantes Virus mit fluoreszierenden Virusproteinen, die den Infektionsstatus einer infizierten Zelle ablesen lassen. Zu diesem Zweck habe ich red fluorescent protein (RFP) an den C-terminus von UL47 fusioniert, einem Protein, das nur während der lytischen Replikation exprimiert wird; und green fluorescent protein (GFP) an den C-terminus von Meq, einem Protein, das währen der Latenz und in transformierten Zellen gebildet wird (vUL47-PRF_Meq-GFP). *In vitro* replizierte vUL47-PRF_Meq-GFPvergleichbar mit dem parentalen Virus und die Expression der fluoreszierenden Proteine konnte beobachtet werden. Interessanterweise verursachte vUL47-PRF_Meq-GFP keine MD, was darauf hindeutet, dass durch die Fusion von GFP and Meq dessen Funktion in der Transformation und Tumorigenese stark beeinträchtigt wird.

Data from this thesis was published in Journal of Virology:

Title:

Marek's Disease Viral Interleukin-8 Promotes Lymphoma Formation through Targeted Recruitment of B Cells and $CD4^+$ $CD25^+$ T Cells

Author:

Annemarie T. Engel, Ramesh K. Selvaraj, Jeremy P. Kamil, Nikolaus Osterrieder, Benedikt B. Kaufer

Publication:

Journal of Virology

Publisher:

American Society for Microbiology

Date:

Aug 15, 2012

Table of Contents

List of Figures and Tables

Abbreviations

BAC	Bacterial artificial chromosome
BSA	Bovine serum albumin
bZIP	Basic leucine zipper protein
cDNA	Copy DNA
CEC	Chicken embryonic cell
DNA	Deoxyribonucleic acid
dpi	Days post infection
EBV	Epstein-Barr virus
E.coli	Escherichia coli
Exp-1	Experiment 1
Exp-2	Experiment 2
FCS	Fetal calf serum
Fig.	Figure
GFP	Green fluorescent protein
HCMV	Human cytomegalovirus
HHV6A/B	Human herpesvirus A/B
HSV	Herpes simplex virus
HVT	herpesvirus of turkeys
IL-8	Interleukin-8
IR_L/IR_S	Internal repeats long / internal repeats short
KSHV	Kaposi's sarcoma-associated herpesvirus
kbp	kilo base pairs
LATs	Latency associated transcripts
MCMV	Murine cytomegalovirus
MEM	Minimal essential medium
Meq	Oncogene located in the **M**DV **E**coRI-**Q** fragment
MHC	Major histocompatibility complex
mini-F	Minimal fertility factor
miRNA	Micro RNA
mTMR	Multiple telomeric repeat
MDV	Marek's disease virus
MD	Marek's disease
ORF	Open reading frame
OriLyt	Origin of lytic replication
PBMC	Peripheral blood mononuclear cell
PF4	Platelet factor 4
pfu	Plaque forming unit
R_L	Repeats long
RFLP	Restriction fragment length polymorphism
RFP	Red fluorescent protein
RNA	Ribonucleic acid
RT	Room temperature
TERT	Telomerase reverse transcriptase
TR_L	Terminal repeats long
TR_S	Terminal repeats short
U_L/U_S	Unique long / unique short

vIL-8	Viral Interleukin-8
vTR	Viral telomerase RNA
VZV	Varicella-zoster virus

1 Introduction

1.1 Herpesviruses

The name Herpes is derived from ancient Greek 'herpein' meaning 'to creep' and was given due to the recurring nature of lip blisters upon herpes simplex virus (HSV) infection. Herpesviruses are included in the order *Herpesvirales* that contains three families, *Herpesviridae Alloherpesviridae* and *Malacoherpesviridae*. Members of the *Herpesviridae* infect a plethora of mammalian and avian species. Viruses of the *Alloherpesviridae* infect amphibians and reptiles, while bivalves are the hosts of *viruses of the Malacoherpesviridae* (Pellet P.E., 2007). Herpesvirus genomes greatly vary in size and are in between 108 -250 kilo base pairs (kbp) in length (Davison *et al.*, 2002). Structurally, herpesvirus virions consist of an icosahedral nucleocapsid surrounding the double stranded linear DNA genome. The nucleocapsid is surrounded by the tegument, a protein layer containing viral and host proteins, and a lipid envelope containing viral glycoproteins which mediate binding to receptors for entry of the virus into the host cell (Fig. 1) (Pellet P.E., 2007).

All herpesviruses possess a set of core genes that can be used to determine a common ancestor, dating back more than 200 million years (Davison *et al.*, 2002). These core genes are usually responsible for the basic viral life cycle including DNA replication, capsid assembly, DNA packaging and nuclear egress. In addition to core genes, each herpesvirus harbors accessory genes necessary for the optimal adaption to its respective biological niche (Davison *et al.*, 2002). These genes can greatly differ between viruses and are sometimes only present in one virus species. In general, accessory genes are grouped into four categories; i) genes that possess immunomodulatory functions and allow the virus to evade host immune response, ii) genes that manipulate the cellular machinery and modulate host cell protein synthesis, iii) genes that are responsible for cell and host tropism of the virus and iv) genes that contribute to the establishment and maintenance of latency in a specific cell type (Davison *et al.*, 2002). Although latency is a common feature of all herpesviruses where only few or no viral genes are transcribed and the virus genome is maintained in the infected cell. Reactivation can occur either spontaneously or upon certain stimuli such as stress, resulting in lytic replication. The means by which latency is established and reactivation is induced differs between herpesviruses and are not well understood (Davison *et al.*, 2002).

Members of the *Herpesviridae* are classified into three different subfamilies, alpha-, beta-, and gammaherpesviruses. Alphaherpesviruses usually have a fast replication cycle, infect

multiple cell types and often more than one host. Latency is predominantly established in sensory ganglia. The human herpesviruses Herpes simplex virus type 1 (HSV-1) and 2 (HSV-1), Varicella Zoster Virus (VZV) as well as a number of animal herpesviruses such as Equine herpesvirus 1 (EHV-1) and Marek's disease virus (MDV) are members of alphaherpesvirinae. The subfamily of betaherpesviruses contains all cytomegaloviruses as well as Human Herpesvirus 6 (HHV6) and 7 (HHV7), which have a rather slow replication cycle and are restricted to one host species. The prototype for the betaherpesvirinae is the human cytomegalovirus (HCMV). Cytomegaloviruses are named after the characteristically enlarged cells that appear during virus infection. Latently infected cells are found in different tissues and cell types including secretory glands and lymphoreticular cells. Gammaherpesviruses are characterized by their tropism for lymphatic cells, in which the viruses establish latency and a tightly restricted host and cell type range. Representatives of this subfamily are Epstein-Barr virus (EBV), and Kaposi Sarcoma Herpesvirus (KHSV) (Pellet P.E., 2007).

1.1.1 Life cycle of alphaherpesviruses

Over the years, the alphaherpesvirus life cycle has been extensively studied using HSV-1 and pseudorabies virus (PRV) as a prototype (Fig. 2). In general, the virus enters a susceptible host cell by fusion of the viral envelope with the cell membrane, thereby releasing the nucleocapsid into the cytoplasm (Fig. 2A). Once in the cytosol, the nucleocapsid is transported along microtubules to the nucleus (Fig. 2B). At the nuclear membrane, the virion docks to a nuclear pore and releases viral DNA into the nucleus, where viral transcription and DNA synthesis takes place (Fig. 2C-E). Unit length viral DNA is then packaged into procapsids producing nucleocapsids (Fig. 2F), which subsequently bud through the nuclear membrane into the cytoplasm (Fig. 2G-I). To produce mature viral particles, nucleocapsids acquire the tegument and obtain their envelope at the trans-Golgi networks (Fig. 2J), from where viral particles are transported to the cell surface and are released from the infected cell (Fig 2K-M) (Mettenleiter *et al.*, 2009).

More specifically, to enter a host cell, viral glycoproteins embedded in the envelope are required. For most alphaherpesviruses, initial attachment is mediated via glycoprotein C (gC) binding to glycosaminoglycanes followed by the binding of glycoprotein D (gD) to cell surface receptors, such as nectins, HVEM, MHC and integrins, depending on the virus species (Spear and Longnecker, 2003). While gD is absent in the highly cell-associated VZV, gD expression is downregulated in almost all cell types for MDV except in the feather follicle epithelium (Niikura *et al.*, 1999; Tan *et al.*, 2001).

Fusion of the viral and host cell membrane is orchestrated by the glycoproteins H (gH) and L (gL) and the fusion protein glycoprotein B (gB) and varying other factors (Campadelli-Fiume *et al.*, 2007). In addition, entry can also occur upon endocytosis of the virion. The decision if the virus enters by fusion or by endocytosis mostly depends on the cell type (Heldwein and Krummenacher, 2008). Upon entry of the virus the capsid is released into the cytoplasm and subsequently transported to the nucleus along microtubules. The capsid then docks to the nuclear pore complex and the virus genome is injected into the pore where transcription initiation might support translocation of the viral genome to the nucleus (Liashkovich *et al.*, 2011). The transactivator VP16 delivered to the infected host cells as a component of the tegument initiates immediate early transcription via the recruitment of cellular transcription factors. Thereby, a gene expression cascade is set off by the expression of immediate early (α) genes including ICP0, ICP4 and ICP22. For expression of the immediate early genes, no de novo synthesis of viral genes is necessary. Expression of immediate early genes, especially ICP4, is required to facilitate expression of early (β) genes which are mainly involved in viral DNA replication. Late gene (γ) expression is stimulated by DNA replication (Boehmer and Nimonkar, 2003; Roizman, 2007). Viral DNA replication is initiated at the lytic origin of replication (*OriLyt)* as a bi-directional replication. If multiple *OriLyt* are present in the virus genome, replication can be initiated at either origin (Bataille and Epstein, 1995). Replication subsequently switches to a rolling circle (sigma) replication, which leads to the synthesis of long head to tail concatemers (Boehmer and Nimonkar, 2003). Intra- and intermolecular recombination that occurs at a high frequency results in branched viral concatemeric DNA (Roizman, 1979). Furthermore, recombination events and branching may support isomerization of the virus genome. This is supported by infection experiments with a single infectious particle, resulting in mixed isomer genome populations within the plaque (Bataille and Epstein, 1995; Roizman, 1979). The a sequences could be identified as recombination hot spots, possibly because endonuclease G causes double strand breaks at these sites (Boehmer and Nimonkar, 2003). Finally, concatameric DNA is cleaved and packaged by a mechanism highly conserved among all herpesviruses into the pre-assembled capsid (Roizman, 2007). Assembled capsids acquire a primary tegument at the inner lamina of the nuclear membrane, including the conserved proteins UL31 and UL34 that facilitate budding through the inner lamina of the nuclear membrane (Mettenleiter *et al.*, 2006). This budding process results in enveloped perinuclear virions (Fig. 2H) differing in their composition from mature extracellular virions or cytoplasmatic viral particles. Enveloped perinuclear virions subsequently fuse with the outer leaflet of the nuclear membrane thereby

releasing the capsid into the cytoplasm. Through interaction of different tegument proteins including UL36, UL37 and UL49 virions further mature in the cytoplasm (Mettenleiter, 2006). Tegument proteins on the one hand interact with capsid proteins via UL36 and on the other hand mediate contact to the cytoplasmatic tails of glycoproteins such as gE/gI, gM or gN via UL49. The virus obtains its final envelope by budding into trans-Golgi vesicles. Vesicles containing virions are then transported to the cell surface where mature virions are released from the host cell (Mettenleiter, 2002).

1.1.2 Genetic system for herpesvirus mutagenesis

Virus genetic systems facilitate the characterization of genes and sequence elements in the virus and are a crucial research tool in virology. Manipulation of large DNA viruses such as herpesviruses has been an obstacle for many years. Bacterial artificial chromosomes (BAC) provided an excellent solution as they can incorporate up to 300kbp DNA and allow maintenance and manipulation of the large virus genome. BACs are based on the minimal fertility factor (mini-F) and are maintained in *E.coli.* Many well-established mutagenesis systems are available (Tischer and Kaufer, 2012) in *E.coli* that are mainly based on homologous recombination systems such as RecA or Red (Tischer and Kaufer). The Red recombination system derived from bacteriophage λ consists of alpha (exonuclease), beta (single strand binding protein), and gam (protecting DNA from degradation), which together mediate site specific homologous recombination (Tischer and Kaufer, 2012; Tischer *et al.*, 2006a). An especially advantageous strategy derived from the Red recombination system is the *en passant* mutagenesis (Tischer *et al.*, 2006a). In the first step, a PCR product containing the desired mutation, a positive selection marker (PS), an adjacent I-SceI cleavage site and sequences at the end of the PCR product that are homologous to the target site in the virus genome in the BAC. The PCR product is incorporated at the target site via homologues recombination and positive bacteria clones are selected. PS is scarlessly removed by the induction of the I-SceI restriction enzyme, which is encoded in the bacterial strain used for the mutagenesis, that cleaves the I-SceI restriction site and allows linearization of the recombinant BAC clone. Upon linearization, a second homologous recombination event facilitates excision of the marker. All in all, *en passant* mutagenesis is a highly efficient tool to introduce mutations into viral genomes maintained in BAC.

1.2 Marek's Disease Virus

1.2.1 History

Marek's disease (MD) was first described by the Hungarian veterinarian Joszef Marek as fowl paralysis in 1907 (Marek, 1907). Over the next decades, MD belonged to a disease complex referred to as avian leucosis, which lead to controversial research results in the field. At the same time, the picture of MD symptoms changed from the classical paralysis induced by lymphomatous nerve infiltrations to more pronounced lymphoma formation in the visceral organs (Biggs, 2004). In the 1960s, MDV, a highly cell associated herpesvirus, was identified as the causative agent of MD by Biggs and colleagues, allowing a separation of the avian leucosis disease complex in MD and avian leucosis (Biggs, 2004; Churchill and Biggs, 1967). Identification of MDV facilitated the rapid development of successful vaccines that represent the first effective vaccines against virus-induced cancer in 1970 (Bublot, 2004; Churchill *et al.*, 1969; Pastoret, 2004). However, over the last decades the clinical picture of MD changed dramatically. Through intensified poultry production and introduction of vaccination programs, more virulent virus strains evolved that can overcome the vaccine protection and cause high economic losses to poultry industry worldwide. Therefore, development of next generation vaccines is necessary that requires a deeper understanding of MDV pathogenesis to develop new vaccination strategies (Davison and Nair, 2005; Gimeno, 2004; Jarosinski *et al.*, 2006; Osterrieder *et al.*, 2006).

1.2.2 MDV characteristics and properties

Marek's disease virus, also known as Gallid Herpesvirus 2, belongs to the *alphaherpesvirinae* and the genus Mardiviruses. It has a class E genome that is characterized by a unique long (U_L) and a unique short (U_S) region each flanked by inverted repeats long (TR_L, IR_L) and short (TR_S, IR_S), respectively (Fig. 4B, upper panel) (Pellet P.E., 2007). Four different genomic isomers exist of a virus with a class E genome that only differ in the orientation of U_S and U_L with respect to each other (Roizman, 1979). Within the inverted repeats long R_L the virus harbors cleavage and packaging sites (a-like sequence) (Pellet P.E., 2007; Roizman, 2007). The genome size is about 180kbp and encodes for more than 100 open reading frames (Osterrieder, 2004). According to the severity of disease in vaccinated and unvaccinated animals, MDV strains can be categorized into mild MDV (mMDV), virulent MDV (vMDV), very virulent MDV (vvMDV) and very virulent + MDV (vv+MDV). mMDV shows infiltration of peripheral nerves with lymphomatous cells. Herpesvirus of turkeys (HVT) based vaccines were the first widely used vaccines, followed by the introduction of bivalent

vaccines. The current gold standard in vaccination is Rispens/CVI988, which provides the best protection (Bublot, 2004). HVT vaccines can prevent disease outbreak in m MDV strains, while in the more virulent strains, bivalent vaccines consisting of HVT and gallid herpesvirus 3, an apathogenic virus closely related to MDV, are necessary. vv+MDV strains are characterized by the ability to cause outbreaks in bivalently vaccinated animals (Davison and Nair, 2005; Payne, 2004).

1.2.3 Clinical Picture of Marek's disease

Clinically, virulent MDV strains usually cause lymphomas in visceral organs including liver, heart, kidneys, reproductive tract, spleen, proventriculus, intestines and bursa as early as 3 weeks post infection (Davison and Nair, 2005). Furthermore, lymphoma cells can be found on a regular basis in muscles, skin and in feather follicles (Payne, 2004). In addition, infiltration of peripheral nerves with lymphomatous cells can cause symptoms ranging from transient ataxia to recumbence. Mortality rates can reach up to 100% in unvaccinated, susceptible chickens infected with a highly virulent strain. During the early phase of infection, chickens develop transient immunosupression due to massive lytic replication in B cells. Due to the immunosuppression, chickens are more susceptible to secondary infections with other pathogens (Islam *et al.*, 2002). In Germany, cases of MD need to be reported to the Bundesministerium für Ernährung, Verbraucherschutz und Landwirtschaft, while internationally MD is not an OIE (organization internationale epizootique) listed disease. (Calnek, 1986; Ellis *et al.*, 1981; Islam *et al.*, 2002; Kleven *et al.*, 1972; Schat, 2004).

1.2.4 Marek's disease pathogenesis

MDV is transmitted via infectious aerosols particles that are shed by infected chickens at high levels with their dander (Davison and Nair, 2005). The virus enters its host through the respiratory tract where it is thought to infect macrophages and dendritic cells that transport the virus to lymphoid tissues where viral antigens can readily be detected in B and T cells (Calnek, 2001) (Fig. 3). In general, MDV infection is divided into two phases, an early cytolytic phase and a latent phase, which is eventually followed by a late cytolytic phase (Baigent, 2004). During the early cytolytic phase between 2-7 days post infection (dpi), MDV efficiently replicates in B cells, resulting in a massive amplification of the virus. Infiltration of infected cells into the thymus and bursa cause a severe atrophy of the organ and apoptosis of B cells. In highly virulent strains, atrophy of thymus and bursa can even be fatal for the chicken (Baigent, 2004; Osterrieder *et al.*, 2006). In the absence of B cells e.g. in bursectomized chickens, MDV infection is severely delayed and lymphoma formation is

impaired (Baaten *et al.*, 2009). However, MDV is still able to infect and establish latency in $CD4^+$ T cells in absence of B cells (Schat *et al.*, 1981). Lytic replication in B cells leads to the activation of T cells that can subsequently be infected. In contrast, resting T cells seem to be refractory for infection (Baigent, 2004; Baigent *et al.*, 1998; Shek *et al.*, 1983). Infected T cells have been shown to transport MDV to the skin, where it infects the feather follicle epithelium (FFE) and infectious virions are shed into the environment around day 14 post infection (Carrozza *et al.*, 1973; Johnson *et al.*, 1975).

The second phase is characterized by the establishment of latency around 6-7 days post infection in $CD4^+$ T cells. This coincides with the onset of anti-viral immune response in the infected animals. The latent phase is characterized by the absence of detectable viral antigens that could elicit anti-viral immune response, although reactivation likely occurs continuously in a few cells. Studies in thymectomized chickens suggest that the cell associated immunity plays an important role in controlling MDV infection. The exact regulation and gene products necessary for the transition to and from latency remain elusive. Genes expressed in latently infected cells are likely involved in the establishment and maintenance of latency (Osterrieder *et al.*, 2006) One of these genes is the viral oncogene Meq, a trans-activator from the c-Jun/Fos family which blocks apoptosis and induces latent gene expression. Furthermore, a set of spliced RNAs, the latency associated transcripts (LATs) can be detected in the nucleus of latently infected cells. Lastly, viral telomerase RNA (vTR), an orthologue of the RNA subunit of the telomerase complex, and vIL-8 are expressed during latency (Jarosinski and Schat, 2007). . In susceptible chickens, the latent phase is followed by a late cytolytic phase around day 14-21 post infection, which is likely caused by the reactivation of latently infected cells. It is associated with permanent immunosuppression and lymphoma formation leading to severe bursa and thymus atrophy, inflammation, lymphocyte necrosis and influx of mononuclear cells and heterophils (Jarosinski *et al.*, 2006).

Furthermore, MDV is able to transform $CD4^+$ T cells, mostly expressing an αβ type T cell receptor (TCRαβ) *in vivo*. Although it is almost impossible to discriminate between latently infected and transformed cells, there is evidence that at the end of the cytolytic phase transformed cells expressing high amounts of $CD30^{high}$ are present. Furthermore, an infiltration of MDV antigen negative CD4+ TCRαβ+ T cells starts around 2 weeks post infection. MDV–induced tumor cells analyzed *ex vivo* are characterized by a large set of surface markers which suggest a regulatory phenotype for MDV transformed cells (Shack *et al.*, 2008). So far, only one MDV associated tumor surface antigen (MATSA) could be identified, which is detected by the AV37 antibody and is rarely found on other MDV

infected cells (Burgess and Davison, 2002; Burgess *et al.*, 2004; Shack *et al.*, 2008). In MD-induced tumor cells, the virus genome is found integrated in multiple chromosomes at the host telomeres, a protective structure at the ends of linear chromosomes (Delecluse and Hammerschmidt, 1993; Delecluse *et al.*, 1993). Integration facilitates maintenance of the MDV genome, while it can efficiently mobilize the genome during reactivation and is important for efficient tumor formation. (Kaufer *et al.*, 2011).

1.2.5 MDV tumorigenesis

An MDV lymphoma mainly consists of latently infected $CD4^+$ T lymphocytes. In addition, few B cells, macrophages and other cells are found in the lesions (Calnek *et al.*, 1989). Surprisingly, only few of the T cells within a lymphoma are neoplastically transformed while the majority of the incoming T cells can be attributed to anti-tumor immune responses (Burgess, 2004). Intriguingly, MDV transformed tumor cells resemble activated memory T_H-2 cells with a regulatory phenotype (Burgess and Davison, 2002; Shack *et al.*, 2008). These cells express various cell surface markers including $CD30^{hi}$, $CD25^+$, MHC class I^{hi} and II^{hi}, and $TCR\alpha\beta^+$. Despite extensive research, only one MDV associated tumor specific antigen (MATSA) was found until now, however, the identity of the antigen itself remains unknown (Burgess and Davison, 2002; Shack *et al.*, 2008). MDV transformed cells express high levels of Meq as well as high levels of CD30 resulting in hyperproliferation and inhibition of apoptosis (Burgess *et al.*, 2004). These findings suggest that neoplastic transformation is an early event where infected and transformed T_H-2 cells extravasate and create a local T_H-2 environment with rapidly dividing cells. Other, non-transformed immune cells are recruited and eventually become lytically infected, thereby sustaining the ongoing pro-neoplastic environment. In resistant chickens however, there is evidence that soon after the early invasion of tissues by transformed cells 5-7 days post infection, $CD8^+$ T cells begin to control the expansion of transformed cells, which would result in tumor regression (Burgess, 2004)..

1.2.6 Viral factors involved in tumorigenesis and pathogenesis

A number of viral factors involved in the transformation have been identified; however, the sequence of events leading to immortalization of the cell has remained elusive. The major oncogene of MDV is Meq, a basic leucine zipper protein (bZIP) encoded in the R_L. The bZIP domain of Meq has a high homology to proteins of the Jun/Fos family (Qian *et al.*, 1995). Homodimerization of Meq leads to repression of gene expression, whereas heterodimerization with proteins of the Jun/Fos family is associated with transactivation. Both homo- and

heterodimerization have been shown to be crucial for the development of T cell lymphomas in infected chickens (Levy *et al.*, 2005).

Another factor involved in tumor development is vTR, a homologue of telomerase RNA (TR). As a subunit of the telomerase complex, TR interacts with the telomerase reverse transcriptase (TERT) and provides the template for telomere elongation (Blackburn, 1991). vTR is able to reconstitute telomerase activity in the cellular telomerase complex in absence of TR and therefore represents a fully functional TR homolog (Fragnet *et al.*, 2003; Fragnet *et al.*, 2005). Deletion of a conserved region 1-2 and 1-4 of vTR in the highly virulent RB-1B strain resulted in highly reduced lymphoma formation, less dissemination and smaller lymphomas (Trapp *et al.*, 2006). Intriguingly, vTR possesses tumor promoting functions that are independent of its function in the telomerase complex. vTR interacts with other proteins such as RPL22, a protein involved in T cell development (Kaufer *et al.*, 2010). A third factor also located in the repeat long regions is RLORF4. Deletion of RLORF 4 severely impairs lymphoma *in vivo*, indicating that RLORF4 is involved in tumorigenesis. Furthermore, non-oncogenic, attenuated MDV strains often harbor deletions in RLORF4, underlining its importance in MDV pathogenesis. However, neither the gene product nor the mechanism have been investigated in detail so far (Jarosinski *et al.*, 2005).

Apart from the proteins involved in MDV pathogenesis and oncogenesis, MDV has recently been shown to encode at least 14 micro RNAs (miRNA), some of them with a potential role in tumor formation (Burnside *et al.*, 2006; Morgan *et al.*, 2008). miRNAs also play a role in tumorigenesis in EBV and KHSV induced cancers and in non-virus induced cancers REF. Overexpression of the cellular miR-155 has already been associated with a variety of cancers (Burnside *et al.*, 2006; Morgan *et al.*, 2008). MDV encodes a miR-155 orthologue called miR-M4, which is highly expressed in MDV induced lymphoma cells. Deletion of the whole miRNA cluster containing miR-M4 completely abolishes tumor formation in infected chickens (Zhao *et al.*, 2009). Point mutations in the seed sequence of miR-M4 reduced tumor incidence in infected animals. Furthermore, miR-155 can complement the function of miR-M4 to a large degree in MDV pathogenesis (Zhao *et al.*, 2009). Besides the gene products involved in MDV pathogenesis, the virus genome harbors two sets telomeric repeat sequences (TMR), short and multiple telomeric repeats (sTMR and mTMR) in the virus genome. The exact TMR sequences as well as mTMRs are dispensable for lytic MDV replication *in vitro*. However, mutation of the viral TMR sequences or absence of the TMR results in a severely reduced disease and tumor incidence in infected animals (Kaufer *et al.*, 2011). Furthermore, MDV TMRs were shown to facilitate targeted integration

of MDV into the host telomeres, a mechanism that allows maintenance of the viral genome in latently infected or transformed cells.

1.2.7 Chicken chemokines and viral Interleukin-8

A common feature of viruses is their ability to modulate the host immune system in order to replicate and spread to the next host. Therefore viruses have evolved numerous strategies to evade and subvert the immune system towards more favorable conditions for virus infection (Tortorella *et al.*, 2000). Strategies to achieve this essential goal range from antigenic variability to targeting cellular pathways such as the interferon, cytokine and chemokine system. Especially Herpes- and Poxviruses encode a variety of genes in their large DNA genome that manipulate the host immune system. They often use viral mimicry of host genes optimized for the benefit of the virus to subvert their host's immune system (Alcami and Koszinowski, 2000).

A number of viral chemokines (virokines), and viral cytokine receptors (viroreceptors) have been described so far. Several viral chemokines and chemokine receptors have been proposed to recruit target cells for infection, block antiviral immune responses or increase host cell and virus replication (Alcami, 2003). For instance, the CXC receptor ORF74 of Kaposi's sarcoma-associated Herpesvirus induces cell proliferation and Kaposi sarcoma-like lesions in a transgenic mouse model (Alcami and Koszinowski, 2000; Arvanitakis *et al.*, 1997; Pati *et al.*, 2001). In human (HCMV) and mouse cytomegaloviruses (MCMV), a number of viral chemokine agonists and antagonists have been described. HCMV UL146 attracts neutrophils while MCMV MCK-1/2 induces chemotaxis in monocytes increasing monocyte associated viremia *in vivo* (Alcami and Koszinowski, 2000). However, it is often difficult to predict the impact of the virokines and viroreceptors in pathogenesis due to the lack of suitable animal models for most of these viruses (Alcami, 2003). In contrast to beta- and gammaherpesviruses, alphaherpesviruses usually do not encode viral chemokines with the exception of MDV (Van de Walle *et al.*, 2007). Therefore, the MDV encoded CXC chemokine vIL-8 is not only unique for alphaherpesviruses, but also provides unique opportunity to study the role of a virokine in pathogenesis using a well-established natural animal model.

Chemokines are small, soluble cytokines with chemotactic properties. They are characterized by four conserved cysteine residues. Positioning of two of the cysteine residues defines the 4 subgroups of chemokines. Cysteine residues 2 and 3 are adjacent in CC chemokines, interspaced by one amino acid in CXC chemokines and interspaced by 3 amino acids in CX_3C chemokines. The fourth subgroup does not have the second cysteine residue

(XC type). Functionally, chemokines recruit leukocytes to various target tissues for either homeostatic or inflammatory purposes (Campbell and Butcher, 2000; Mackay, 2001). In order to migrate from the blood stream towards the target tissue, leukocytes use a diapedesis mechanism. Diapedesis is initiated by leukocytes rolling on the endothelial surface where they finally attach. To arrest the cells on the endothelial surface prior to emigration, integrins receptors on the surface of the leukocyte bind to ligands including intercellular adhesion molecules (ICAMs), vascular cell adhesion molecule 1 (VCAM-1) and mucosal addressin cell adhesion molecule 1 (MAdCAM-1) on the vascular endothelium (Cinamon *et al.*, 2001a; Cinamon *et al.*, 2001b). Finally, both shear forces and chemokines bound to the apical surface of endothelial cells are necessary to induce transmigration (Cinamon *et al.*, 2001b). Thus it is conceivable that a virus exploits this mechanism for the recruitment of target cells by the secretion of viral chemokines from infected cells.

CXC chemokines surprisingly have a rather conserved structure despite the manifold specific functions they have (Strieter *et al.*, 1995). The unstructured N-Terminus is generally associated with receptor specificity and a number of studies investigated the ELR motif directly preceding the CXC box that is present in many CXC chemokines (Clark-Lewis *et al.*, 1991; Hebert *et al.*, 1991). ELR is supposedly responsible for neutrophil chemotaxis and introduction of ELR into ELR negative CXC chemokines significantly increased chemotaxis of neutrophils (Clark-Lewis *et al.*, 1993). Studies on other motifs in the N-terminus are scarce so far.

Furthermore, chemokines are well characterized tumorigenesis promoting factors (Mukaida and Baba, 2012). One mechanism supporting tumor formation is the pro-angiogenic function found in some chemokines such as IL-8 (Waugh and Wilson, 2008). For other chemokines such as platelet factor 4 (PF4), angiostatic properties could be demonstrated (Maione *et al.*, 1990). In some studies functions of these chemokines in angiogenesis were mapped to the C-terminus (Maione *et al.*, 1990; Sharpe *et al.*, 1990).

In chickens, 8 CXC chemokine orthologues have been identified so far. Functions for most of the chicken CXC chemokines except for CXCLi1 and CXCLi2 are poorly understood and mostly deduced from mammalian homologues (Kaiser *et al.*, 2005). Especially chemokines involved in inflammatory responses are generally thought to recruit immune cells to the site of inflammation. Two of the inflammatory chemokines, CXCLi1 (K60) and CXCLi2 (9E3/CEF4 or CAF) are proposed to be the orthologues of human IL-8 (CXCL8). CXCLi3 has no designated counterpart in mammals and its function is unknown (Kaiser *et al.*, 2005) The other 5 CXC chemokines belong to the homeostatic group, which maintain and

coordinate leukocyte trafficking throughout the body. It includes a CXCL12, a CXCL14 orthologue, and chCXCL13L1, chCXCL13L2 and CXCL13L3, three orthologues of mammalian CXCL13 (Kaiser *et al.*, 2005; Kaiser *et al.*, 2009). Mammalian CXCL13 is a B cell homing chemokine recruiting B cells to priming sites and lymphatic tissues, where it is expressed by non-lymphoid cells (Cyster *et al.*, 2000). Initially, the MDV chemokine vIL-8 was reported to be an IL-8 orthologue that was pirated from the chicken genome (Kaiser *et al.*, 2005; Parcells *et al.*, 2001). However, based on sequence comparison after completion of the chicken genome project, the MDV CXC chemokine vIL-8 was found to have highest sequence homology to CXCL13 (B. Kaspers, personal communication) (Staeheli *et al.*, 2001). Currently, collaborators are elucidating the function of CXCL13 homologues in the B cell development of the chicken. Due to the high similarity of vIL-8 to CXCL13, vIL-8 was included in some studies showing that vIL-8 uses the same receptor (CXCR5) as host B cell chemokines (B. Kaspers, unpublished data). Intriguingly, CXCR5 in mammals is not only expressed on B cells, but also on some memory T cells and activated T cells, which upregulate the receptor upon activation (Ansel *et al.*, 1999; Cyster *et al.*, 2000).

Previous studies on vIL-8 have demonstrated that deletion of the entire *vIL-8* ORF severely affects MDV pathogenesis and significantly reduces tumor incidence by about 90% in infected chickens (Cui *et al.*, 2004; Parcells *et al.*, 2001). In addition, vIL-8 deletion mutants showed reduced viral replication in lymphoid organs at 6dpi, suggesting a role of vIL-8 during lytic replication (Cui *et al.*, 2004). However, transmission of the virus did not seem to be reduced as the vIL-8 deletion mutant replicated in feather follicle epithelium to the same extent as wild type virus and induced anti-MDV antibody formation in naïve contact birds (Cui *et al.*, 2004). Following these initial reports, a number of splice variants were identified that contain vIL-8 exons II and III fused to the major oncogene Meq, and to other upstream genes, including ORF4 and ORF5a (Fig. 4A). These splice products, which lack the vIL-8 signal peptide, are expressed within infected cells *in vitro* and *in vivo* (Jarosinski and Schat, 2007), demonstrating the complexity of transcription in this genomic region. Functionally and despite being designated an IL-8 orthologue, vIL-8 showed chemotactic properties for PBMCs *in vitro* suggesting that vIL-8 could recruit target cells for infection (Parcells *et al.*, 2001). Yet the exact target cell population explaining the mechanism by which vIL-8 supports lymphomagenesis remained unknown.

Understanding the functions of vIL-8 will not only characterize a virulence factor in MDV pathogenesis and tumorigenesis but also provide insights into important functions and roles of chemokines in the avian immune system.

1.3 Project introduction

1.3.1 Generating a tool (pΔIR$_L$) for manipulation of diploid genes within the repeats long of MDV

Manipulation of diploid genes present in the inverted R_L of MDV using homologous recombination techniques has always been a challenge (Fig 4B, genome structure). Two rounds of mutagenesis including laborious screening procedures were needed to mutate both gene copies in the MDV genome. Furthermore, it was difficult to determine which gene locus has already been targeted in the first round of mutagenesis, especially when point mutations were introduced to address the function of specific motifs. In addition, long homologous sequences often enhance targeting the already mutated locus again during the second mutagenesis round where recombination occurs with a higher efficiency due to the higher sequence homology. To circumvent these problems, my aim was to construct a virus with a deletion of almost the entire R_L sequences in one locus based on an infectious BAC of the very virulent RB-1B strain (pΔIR$_L$). Using pRB-1B as a platform, only one round of mutagenesis was necessary to introduce mutations into genes encoded in the R_L. Upon MDV reconstitution from BAC DNA, the deletion was efficiently restored by intra- and intermolecular recombination events during herpesvirus replication (see section 1.1.1). Restoration of the deletion upon reconstitution introduces any mutation in the TR_L into the IR_L.

1.3.2 The role of viral Interleukin-8 in MDV pathogenesis

Using ΔIR$_L$ as a tool allowed me to modify the diploid vIL-8 gene in the R_L; I investigated if and how the secreted chemokine vIL-8 contributes to MDV pathogenesis. Previous studies have demonstrated that deletion of the entire *vIL-8* ORF severely affects MDV pathogenesis and significantly reduces tumor incidence by about 90% in infected chickens (Cui *et al.*, 2004; Parcells *et al.*, 2001). Following these initial reports, a number of splice variants were identified that contain vIL-8 exons II and III fused to the major oncogene Meq, and to other upstream genes, including ORF4 and ORF5a. These splice products, which lack the vIL-8 signal peptide, are expressed within infected cells *in vitro* and *in vivo* (Jarosinski and Schat, 2007), demonstrating that the complexity of the transcription in this genomic region. Hence, my aim was to investigate the role of vIL-8 in MD pathogenesis and tumorigenesis in the presence of splice variant expression.

Functionally and despite being designated an IL-8 orthologue, vIL-8 showed chemotactic properties for PBMCs *in vitro* suggesting that vIL-8 could recruit target cells for infection.

However, the exact target cell population explaining the mechanism by which vIL-8 supports lymphomagenesis remained unknown. To understand the mechanism, how a viral chemokine can influence pathogenesis, I wanted to identify target cells for vIL-8 to understand the mechanism by which vIL-8 promotes MD. For ELR^+ CXC chemokines it is well-established that the ELR motif is responsible for receptor specificity and neutrophils recruitment (Clark-Lewis *et al.*, 1991; Hebert *et al.*, 1991). Therefore, my aim was to investigate if the DKR motif similar to the ELR motif contributes to the receptor specificity. Furthermore, Parcells and colleagues (Parcells *et al.*, 2001) suggested, that vIL-8 might be involved in neovascularization of MDV induced tumors. Studies on CXC chemokines in tumorigenesis have suggested that the C-terminus has either angiogenic or angiostatic properties (Maione *et al.*, 1990; Strieter *et al.*, 1995). Hence, I wanted to elucidate whether vIL-8 C-terminus has tumor promoting functions, for example by increasing angiogenesis in MDV induced lymphomas.

1.3.3 Generation of a markervirus for latency

For about 30 years, the model of the MDV life cycle proposed by Calnek and Schat (Calnek, 1986) has mostly remained unchallenged. Understanding when and in which cells and tissues a herpesvirus replicates lytically or resides latently could therefore provide further insight into the pathogenesis of Marek's Disease. However, it has remained difficult to discern lytic and latent infection *in vivo*. To shed light onto the infection status of cells and tissues *in vivo*, the goal was to generate a markervirus for lytic and latent infection. . Previously, fluorescent tagging of UL47, a capsid protein expressed only during lytic infection, resulted in a markervirus for lytic infection without affecting pathogenesis and tumorigenesis *in vivo* (Jarosinski *et al.*, 2012). To visualize latently infected cells I inserted a green fluorescent protein (GFP) at the C-terminus of Meq, which is highly expressed in latently infected and transformed cells and only to a low extent during lytic infection. The aim was, to generate and characterize vUL47-RFP_Meq-GFP to obtain new insights into the MDV life cycle.

2 Materials and Methods

2.1 Materials

2.1.1 Buffers

Buffers for mini- and midi preparation of DNA

P1 buffer	pH 8.0	P2 buffer		P3 buffer	pH 5.5
50m M	Tris-Cl	200mM	NaOH	3M	K acetate
10mM	EDTA	1%	SDS		
(100µg/ml	RNase A)				

Southern blotting buffers

Transfer buffer		10X SSC	pH 7.0	High stringency buffer	
0.5M	NaOH	175.3g	NaCl	2x	SSC
1.5M	NaCl	88.2g	Na citrate	0.1%	SDS

Low stringency buffer		5x Maleic Acid buffer pH7.4		Southern I	pH 7.5
0.5x	SSC	58.05g	Maleic acid	0.1M	Maleic acid
0.1%	SDS	43.82g	NaCl	0.15M	NaCl
		36-40g	NaOH		

Southern II		Southern III		Church buffer	
1x	Maleic acid buffer	0.1M	Tris-HCl	1%(v/v)	bovine serum albumin
1%	blocking reagent	0.1M		1mM	EDTA
				0.5M	Phosphate buffer*
				7%(w/v)	SDS
				*Phosphate buffer	
				134g	$Na_2HPO_4x7H_2O$
				4%(w/v)	85% H_3PO_4

Protein electrophoresis and Western blotting buffers

10X SDS running buffer		Cathode buffer		Anode Buffer I	
10%	SDS	25mM	Tris	300mM	Tris
30.3g	Tris	10% (v/v)	Methanol	10% (v/v)	Methanol
144.1g	glycine				

Anode buffer II	Coomassie brilliant blue	

25mM	Tris	7% v/v	acetic acid		
10% (v/v)	Methanol	50% v/v	methanol		
40mM	amino hexane acid	0.25% w/v	Coomassie R-250		

Protein G affinity purification buffers

binding buffer pH 7.0		elution buffer pH 2.7		10x PBS	pH 7.0
20mM	NaH_2PO_4 x H_2O	0.1M	glycine	80g	NaCl
				2g	KCL
				26.8g	Na_2HPO_4 x $1H_2O$
				7.4g	Na_2EDTA

Other buffers

2x HBS buffer for Ca-Phospate transfection pH 7.05		50x TAE	pH 8.0	Digestion buffer for DNA extraction (eukaryotic cells)	
140mM	NaCl	242g	Tris	100mM	NaCl
1.5mM	Na_2HPO_4 x $2H_2O$	57.1ml	glacial acetic acid	10mM	Tris-Cl (pH 8.0)
50mM	HEPES	100ml	0.5M Na_2EDTA	25mM	EDTA
				0.5%	SDS

2.1.2 Media and buffers for cell culture and bacteria culture

Cell culture media

MEM complete		minimal MEM		freezing MEM	
500ml	MEM	500ml	MEM	100ml	MEM complete
10% v/v	FCS	0,5% v/v	FCS	8% v/v	DMSO
1% v/v	P/S	1% v/v	P/S		

LM Base		LM Hahn		chemotaxis medium	
500ml	McCoy's 5A	500ml	LM Base	500ml	RPMI 1640
500ml	Leibovitz L15	10% v/v	FCS	0,25 w/v	BSA
100ml	10x Tryptose phosphate broth	8% v/v	chicken serum		
2,6ml	10% Na_2CO_3				
11ml	1mM ß-Mercaptoethanol			P/S	
11ml	NaPyrovate			650mg	Penicillin
11ml	P/S			1g	Streptomycin
11ml	200mM L-Glutamine			100ml	H_2O

bacteria culture

LB	pH 7.0	LB Agar	Chloramphenicol

10g 5g 10g 1000ml Kanamycin	Bacto-Tryptone Bacto-Yeast NaCl H_2O	100ml 2% w/v Ampicillin	LB Agar	34mg 1ml	Chloramphenicol Ethanol
30mg 1ml	Kanamycin H_2O	100mg 1ml	Ampicillin H_2O		

2.2 Generation of mutant viruses.

2.2.1 DNA mini- and midi- preparation

Due to the large similarities, mini- and midi- preparation are described together, where volumes and conditions for midi-preparations indicated in brackets. To isolate BAC and plasmid DNA from E.coli, overnight LB medium cultures 5ml (150ml for BACs, 50ml for plasmids) containing the appropriate antibiotics were inoculated. Plasmids were grown at 37°C unless otherwise indicated. The bacterial strain used for BAC mutagenesis, GS1783 (kindly provided by G. A. Smith, Northwestern University, Chicago, IL), contains a temperature sensitive promoter for the expression of the Red recombination system. GS1783 were therefore grown at 32°C to avoid induction of the recombination system that could result in random recombination during bacteria expansion. Bacterial cultures were grown overnight, transferred to centrifuge tubes and bacteria were pelleted at 5000rpm in 2ml centrifuge tubes (13000rpm in 200ml beakers). Supernatant was removed and bacteria pellets were resuspended well in 300µl (5ml) of P1 buffer, containing 20µg/ml of RNase A (20mg/ml) was added for a midi prep. To lyse the bacteria, 300µl (5ml) P2 buffer was added and tubes were inverted quickly to ensure complete lysis. Then 300µl (5ml) P3 were added to precipitate protein. Samples were centrifuged at maximum speed to remove the protein debris.

For mini preps, the supernatant was then transferred, mixed with 500µl Phenol:Chloroform:Isoamylalcohol 25:24:1 (AppliChem) on the vortex and then centrifuged at maximum speed for 20min. The upper phase was transferred to fresh tubes. For midi preps, the supernatant was transferred to equilibrated midi prep columns (Qiagen) and DNA was allowed to bind to the column material. After washing the column with the supplied wash buffer, DNA was eluted from the column with the elution buffer preheated to 65°C to facilitate the release of the relatively large BAC DNA from the column. Subsequently, the DNA from mini or midi preps was precipitated using 0.7 volumes of isopropanol and then centrifuged at maximum speed for 30min at 4°C to pellet the DNA. The DNA pellet was washed twice with 70% ethanol and then dried before resuspending it in TE

RNase for mini preps and molecular grade water for midi preps. Mini-preps were then incubated for 30min at 37°C to allow the RNase to degrade RNA.

2.2.2 Preparation of electro-competent and recombination competent *E.coli*

An LB culture containing CAM was inoculated with the respective BAC clone and grown overnight at 32°C. This fresh overnight culture was used to inoculate a pre-warmed 50 ml LB culture at a 1:50 ratio and grown for 3-4 h at 32°C to an optical density of 0.5-0.7, indicating that bacteria are in the logarithmic growth phase. The recombination system was induced by a heat shock at 42°C for 15min. Subsequently, cells were immediately cooled using an ice water bath for 20 min. LB medium and excess salts were removed by 2 washes with 50ml sterile, ice-cold 15% glycerol. The bacteria were then resuspended in 250-300µl of 15% glycerol and shock frozen in liquid nitrogen and stored at -80°C until further use or directly used for electroporation.

2.2.3 Generation of pΔIR_L as a tool for manipulation of repeat long genes

pRB-1B, an infectious BAC clone of the highly oncogenic RB-1B MDV strain was used for the generation of pΔIR_L by two-step Red-mediated mutagenesis as described previously (Tischer *et al.*, 2006b). Initially, approximately 10 kbp of the IR_L of pRB-1B were deleted, leaving 0.5 kbp at the left and 1.5 kbp at the right end of the IR_L intact to allow restoration of the sequence via homologous recombination during MDV replication in pΔIR_L (Fig 4B). To generate pΔIR_L, primers (see table 1) containing homologous sequences upstream and downstream of the deletion as well as a sequence duplication that allows removal of the positive selection marker were designed and used to amplify *aphAI*-I-*Sce*I cassette from pEPkanS1. A two-step PCR protocol using Taq polymerase was used, running at a constant extension time of 1:20 min 10 cycles with an annealing temperature of 50°C and 20 cycles with an annealing temperature of 65°C. The resulting PCR product was gel purified using a commercially available gel extraction kit (Qiagen QiaQuick Gel Extraction Kit or SLG HiYield®PCR clean-up/ Gel Extraction Kit) and 50ng of PCR product was electorporated into electro- and recombination competent E.coli strain GS1783 containing pRB-1B (clone 1232). Bacteria were allowed to recover at 32°C for one hour in SOC medium, then plated and grown on LB Agar plates at 32°C containing chloramphenicol and kanamycin for selection of recombinant clones. Clones were picked, inoculated on replica plates and DNA was isolated using mini preps. Using restriction fragment length polymorphism (RFLP) of parental BAC and recombinant clones, CAM/KANA positive clones were screened for the deletion and to ensure integrity of the virus genome. For this purpose, 10 µl (1 µg) BAC DNA

was digested with 10 unit of either restriction enzyme A or B (NEB) for 3-4h at 37°C. Samples were separated on a 0.8% agarose gel at 55V overnight and then visualized using ethidium bromide staining with the Bio-Vision detection system (PeqLab). For the removal of the *aphAI*-I-*Sce*I cassette from correct intermediate clones, overnight cultures of these intermediate clones were grown at 32°C and used to inoculate a 2ml culture containing no kanamycin. When bacterial growth reaches the log phase after approximately 3h, I-Sce-I expression was induced for 1h by adding 2ml LB 2% L-arabinose. Next, the recombination system was induced for 30 min at 42°C and afterwards bacteria are allowed to recover for 1h at 32°C before they were plated at a 10^{-5} dilution on Agar plates. Colonies usually become visible after 24-48h at 32°C. RFLPs were used to identify correct final clones. The mutation sites in correct clones were amplified via PCR from positive clones and sequenced. Correct final clones as well as corresponding intermediates were stored as glycerol stocks at -80°C.

2.2.4 Generation of vIL-8 mutants

In analogy to the construction of pΔIR_L three different vIL-8 mutants were constructed based on pΔIR_L: (1) pΔMetvIL-8, in which the vIL-8 start codon ATG was mutated to TTG; (2) pvIL-8_ELR, in which the conserved neutrophil chemotaxis target motif ELR was introduced, replacing a DKR motif in vIL-8; (3) pvIL-8ΔC-term, in which a premature stop codon was introduced to elucidate a potential function of the long C-terminus of vIL-8 compared to the related cellular 9E3/CEF4, a chicken IL-8 orthologue. Furthermore, for each of these vIL-8 mutants, a revertant, in which the mutation was reverted to the wild type sequence, was generated in order to show that phenotypical changes of the mutant viruses are specific for the introduced mutation and do not result from random mutations in the virus genome during virus construction.

2.2.5 Generation of pUL47-RFP_Meq-GFP

In order to generate a virus expressing fluorescently tagged Meq and UL47, a previously generated virus, pRB-1B-UL47RFP served as a parental virus to generate pUL47-RFP_Meq-GFP (Jarosinski *et al.*, 2012). To tag Meq with GFP, in pRB-1B-UL47-RFP, the internal repeats long were first deleted as for generation of pΔIR_L (see 2.3.3) resulting in pΔIR_L-UL47-RFP. Next, GFP was inserted at the C-terminus of the remaining Meq gene in the TR_L via two step red mediated mutagenesis as described above using the shuttle plasmid pEP-EGFP-in (Brazeau *et al.*), resulting in pUL47-RFP_Meq-GFP.

2.2.6 Southern blotting analysis of the pΔIR$_L$ genome structure

Southern blotting was used to analyze genome integrity and mapping of ΔIR$_L$. DNA from parental pRB-1B and from pΔIR$_L$ was digested with different restriction enzymes and genome fragments were separated on a 0.8% agarose gel at 65V overnight. DNA was visualized with ethidium bromide and picture was taken using the Bio-Vision detection system (PeqLab). After washing the agarose gel in water for 30min, the gel was acidified in 0.25NHCl for 10min for depurination. DNA was transferred onto a positively charged Nytran®SPC membrane (Whatman) overnight using southern blot transfer buffer. The membrane was dried and DNA cross-linked to the membrane by UV exposure for 12s. To visualize specific DNA fragments, the membrane was probed either with a DIG labeled probe specific for the telomeric repeats that are adjacent to the deletion or a probe detecting vIL-8 located in the deleted fragment. Membranes were pre-incubated for 30min at 42°C with church buffer. The probes were then hybridized to the membrane overnight at 50°C (vIL-8) or 55°C (telomeric repeats). Membranes were washed with low stringency buffer twice for 15min at RT followed by two washes with high stringency buffer at 65°C for 15min. To prepare the membrane for detection, it was washed with Southern buffer I for 5min at room temperature, blocked with Southern buffer II for 30min and then incubated with anti-DIG antibody dissolved in Southern buffer II at 1:10000 dilutions for 30min. The membrane was then washed twice in Southern buffer I for 15min and equilibrated in Southern buffer III for 5min prior to adding CPD Star reagent to visualize bands. Signal was recorded using the Chemi-Smart 5100 detection system (PeqLab)

2.3 Cells and viruses.

2.3.1 Preparation and maintenance of chicken embryo cells

Chicken embryo cells (CEC) were prepared from specific-pathogen-free embryos and maintained as described previously (Osterrieder, 1999). For this purpose, eggs were incubated for 11-12 days as described previously (Osterrieder, 1999). Prior to cell preparation, eggs were carefully cleaned with 70% ethanol and then opened. The embryos were taken out of the eggs and head, extremities and inner organs were removed. The remaining embryo was washed in PBS to remove blood and detritus. Remaining tissue was dissociated to obtain small pieces and washed with PBS on a magnetic stirrer for 10min. PBS was carefully discarded after the wash. To release single cells, the tissue was then digested for 10min on a magnetic stirrer in ca. 100ml PBS 0,025% Trypsin. The cell suspension was then removed,

filtered over sterile gauze membrane and collected in MEM complete. Trypsin digest was repeated to dissociate the remaining tissue pieces two more times. Cells were harvested by centrifugation at 300 ×g for 10min at room temperature. The resulting cell pellets were pooled and resuspended in a total volume of 150 ml MEM complete. Quality and concentration of cells was determined using an inverted microscope and the appropriate number of cells plated into tissue culture flasks. To passage CECs, medium was aspirated and cells were washed with PBS. Cells were then incubated with 0.05% trypsin and incubated for 5-10min at 37°C until the cells detached. MEM complete was added to inactivate the trypsin and cells were resuspended and then divided at a 1:2 or 1:3 ratio. CECs were passaged no more than 3 times.

2.3.2 Reconstitution of infectious MDV BACs

For reconstitution of recombinant viruses, CECs were plated into 6-well plates the day prior to transfection to obtain an optimal confluence of 80-90 %. 1µg of MDV BAC DNA was co-transfected with pCAGGS-NLS/Cre, a plasmid encoding Cre recombinase for removal of the mini-F sequence as described previously (Jarosinski *et al.*, 2007a). Briefly, DNA was dissolved in 50µl of 10mM Tris pH 7.5 and the volume adjusted to 438 µl with molecular grade water. This solution was incubated for 30min at RT. 62µl of 2M $CaCl_2$ were carefully added drop wise, while gently shaking the DNA containing tube on a vortexer, and incubated overnight at 4°C. The next day, 500µl of 2x HBS were added drop wise and incubated for 15min at room temperature. The media of the 6-well plates was changed and 500µl of the transfection mix added to each well. After a 3-4 hour incubation the cells were gently washed with PBS, incubated in 1ml warm 1x HBS 15% glycerol for 2min, washed with PBS and then 2ml MEM complete added to each well. Plaque formation could be observed 4-6 days post transfection. (Jarosinski *et al.*, 2007b; Osterrieder, 1999; Schumacher *et al.*, 2000).

2.3.3 Virus propagation

Virus was propagated on CEC for 2-4 passages as described previously. Briefly, CECs were washed with PBS and cells were then incubated with 0.05% trypsin at 37°C for 2-10min until CECs detached. To inactivate the trypsin, cells were resuspended in MEM complete and split 1:2 or 1:3. Infected and uninfected CECs were co-seeded with at an appropriate density and grown to confluence when serum concentration was reduced to 0,5%. Virus stocks were prepared by resuspending and aliquoting highly infected cells in freezing MEM Aliquots were stored in liquid nitrogen until further use.

To titrate virus stocks, infected cells were thawed and 10^{-2} to 10^{-4} dilutions were co-seeded with uninfected CECs in duplicates. After 6 days, cells were washed with PBS and

then fixed using ice-cold 90% acetone and incubated for 10 min at -20°C. Acetone was removed and plates were dried and stored dry until indirect immunofluorescence staining (IFA) as described in 2.3.4 to detect plaques.

2.3.4 Immunofluorescence staining of infected CECs

Immunofluorescence staining was used to visualize infected CECs and plaques in virus titrations, plaque size assays and multi-step growth kinetics. Cells were fixed with ice-cold 90% acetone, dried and then blocked with PBS 1% FCS for 30min. After removing the blocking solution, the cells were stained with anti-MDV chicken serum (1:1000) or mouse anti-pp38 antibody (1:1000) diluted in PBS 1% FCS for 30min. The staining solution was removed and the cells were washed 3x for 5min with PBS 1% FCS. As a secondary antibody, anti-chicken or anti-mouse Alexa Fluor antibodies (1:10000) were applied for 30 min and the cells were washed 3x for 5min with PBS 1% FCS. Plaques were then counted and images taken with Zeiss AxioVert S100 fluorescence microscope.

2.3.5 Growth kinetics and plaque size assays.

Replication properties of recombinant viruses were determined by multi-step growth kinetics as described previously (Schumacher *et al.*, 2005). Briefly, $1x10^6$ CEC cells were infected with 100 plaque-forming units (pfu) of each recombinant virus. At 1, 2, 3, 4, 5 and 6 dpi cells were harvested, titrated on fresh CECs, and fixed after 6 days post titration with 90% ice-cold acetone. Plaques were counted and pfu per ml determined for each time point.
For plaque size assays, $1x10^6$ CEC cells were infected with 100 pfu and fixed at 6 dpi. Fixed cells were stained by indirect immunofluorescence as described above. Images of at least 45 randomly selected plaques were taken and plaque areas determined using Image J software (NIH).

2.3.6 DNA extraction from CECs

Cells were trypsinized and washed in PBS. Cells were resuspended and lysed in digestion buffer and then incubated overnight at 37°C with 100µg/ml Proteinase K. DNA was extracted twice with Phenol:Chloroform:Isoamylalcohol 25:24:1 (AppliChem) and once with Chloroform. To remove RNA from the sample an RNase digest (20µg/ml) was performed followed by DNA precipitation with ethanol at a final concentration of 70%, pelleted by centrifugation and washed with 70% ethanol. The DNA pellet was dried and resuspended in molecular grade water.

2.3.7 Western blotting analysis of vIL-8 expression.

$1x10^6$ CEC were infected with 500 pfu of vΔIR_L, vΔMetvIL-8, or vΔMetvIL-8rev. Supernatants from infected cells were harvested at 6 dpi, resolved on sodium dodecyl sulfate (SDS)-15% polyacrylamide gel electrophoresis (PAGE) gels, and proteins were transferred to a PVDF membrane in a semi dry blot system at 1,2 mA/ cm^2 for 40 min. Membranes were then probed using a polyclonal rabbit anti-vIL-8 antibody diluted 1:5000 or an anti-gC antibody diluted 1:100 in PBS-T 5% skim milk (Cui *et al.*, 2004). Target proteins were visualized using a HRP-conjugated goat anti-rabbit IgG antibody or goat anti-mouse-IgM antibody (Southern Biotech) at 1:10000 dilution in PBS-T 5% skim milk. Enhanced chemiluminescence (ECL) Plus^{TM} western blot detection reagents (Amersham GE Healthcare) were used to visualize the proteins, and signal was recorded using the Chemi-Smart 5100 detection system (PeqLab).

2.3.8 Testing for ΔIR_L repair upon reconstitution of the virus

DNA was extracted from infected cells or tumor cells as described in 2.3.5. To test if the deletion was still present, the deletion site was amplified by PCR using primers specific for sequences upstream and downstream adjacent to the deletion site. pΔIR_L served as a positive and pRB-1B as a negative control. Samples from passages II, III and V after infection and from tumor cells were tested, to see if the fragment containing the deletion was still present in the virus genome. In case there is no deletion present, the PCR fragment would be ~10kb and cannot be amplified with this PCR. As a control for DNA quality, a primer set for vIL-8 was used for this experiment listed in table 1.

2.3.9 Detection of vIL-8 spliced transcripts in vΔMetvIL-8 infected cells

CECs were infected with 1000 pfu per well and harvested after 5 days. RNA was extracted using the RNeazy kit (Qiagen). RNA was transcribed into cDNA using the Avian enhanced RT kit (Sigma Avian enhanced RT kit) using random nonamer primers. To detect vIL-8 spliced transcripts, primers published by Jarosinski and colleagues (Jarosinski and Schat, 2007) (Table 1) were used to detect either vIL-8 spliced and unspliced transcripts or Meq-vIL-8 spliced transcripts.

2.4 *In vivo* experiments

2.4.1 Infection experiments

Chickens were housed in isolation units at 25°C with a 12 hour light program. The chickens were kept in stainless steel cages on sand enriched with straw. Food and water was provided *ad libitum*. Up to 10 days post hatching, one heating plate was provided per cage. One-day old specific-pathogen free Valo chickens per group (Lohmann Tierzucht Germany) were tagged with individual numbers (Swifttack^{TM} for Poultry^{TM}, Heartland Animal Health inc.) and infected *intra abdominally* with 1,000 pfu of either vΔIR$_L$, vΔMetvIL-8, vΔMetvIL-8rev, vvIL-8ΔC-term or vvIL-8ΔC-term rev, or vUL47-RFP_Meq-GFP (Table 2). Virus was titrated again on CECs after infection to determine the minimum infectious dose per chicken. Naïve chickens were housed in the same cage with infected animals to investigate transmission of the virus via the natural route of infection. Chickens were monitored for clinical symptoms of MD on a daily basis. Clinical MD symptoms of an animal served as a termination criteria. Animals were examined for tumorous lesions *post mortem* once clinical symptoms were evident or after termination of the experiments. Experiment #1 (Exp-1) was terminated 63 days and experiment #2 (Exp-2) 91 dpi. Stability of the vIL-8 start codon mutation was confirmed by DNA sequencing of the vIL-8 locus derived from vΔMetvIL-8 induced tumors.

2.4.2 Quantification of MDV genome copies in chicken whole blood.

Blood samples (40µl) were taken from the wing vein of infected animals at 4, 7, 10, 14, 21 and 28 dpi and from contact animals at 35 and 40 dpi to determine MDV genome copies in the blood. 40µl of blood were mixed with 20µl 100mM EDTA and stored at -80°C until further use. DNA was isolated from 10µl of the blood using the E-Z96 96-well blood DNA isolation kit (Omega Biotek USA) according to the manufacturer's instructions.

For the qPCR reaction a master mix was set up containing 10µl Master Mix (PerfeCTa®qPCR Fast Mix® UNG low ROX, Quanta Biosciences inc.), 0.12µl of each primer (100µM) and 0.5µl probe (10µM) per reaction and 9.5µl of DNA sample was added. MDV genome copies were determined by quantitative PCR (qPCR) on a 7500 Fast Real-Time PCR System (Applied Biosystems) using specific primers and probe for the MDV ICP4 gene. ICP4 gene copy numbers were normalized against cellular genome copies of the inducible nitric oxide synthase (iNOS) gene as described previously (Jarosinski *et al.*, 2007a).

2.4.3 Isolation of tumor cells from solid organ tumors

To isolate tumor cells from solid organ tumors, tumors were extracted upon euthanasia of the animals. Single cells were prepared from the tumor by mincing the tumor tissue through a cell strainer (BD Falcon) with PBS. Cells were harvested by centrifugation and the cell pellet resuspended in an appropriate volume of PBS. Tumor cells were then purified using a Bicoll gradient (1.077g/ml, Biochrom). Cells were washed with PBS and then either frozen or transferred to cell culture dishes in LM Hahn medium. Conditioned LM Hahn medium was occasionally used to support the adaption of the tumor cells to *in vitro* conditions (Calnek *et al.*, 1989; Calnek *et al.*, 1981).

2.5 *In vitro* characterization of vIL-8

2.5.1 Construction of vIL-8, vIL-8_ELR and vIL-8ΔC-term pFastBac transfer plasmids

Recombinant vIL-8 protein was generated using the Bac-to-Bac baculovirus expression system (Invitrogen). Briefly, recombinant bacmids were generated using the pFastBac Bac-to-Bac system, according to the manufacturer's instructions. The vIL-8 transfer plasmid was constructed to allow expression of vIL-8 as a secreted protein containing a C-terminal tag comprised of the Fc region of human immunoglobulin G (IgG) followed by a polyhistidine motif (6×His). To generate the transfer plasmids for expression of vIL-8-Fc-His, vIL-8_ELR-Fc-His and vIL-8ΔC-term-Fc-His, the vIL-8 cDNA was first amplified by PCR and cloned into the CpoI site of pFastBac11-Cpo-Fc-His, a derivative of pFastBac11-Cpo-His (Van de Walle *et al.*, 2007), which incorporates an IgG Fc cDNA from pcDNA-IgG Fc (a generous gift of O. Negrete and B. Lee, University of California Los Angeles, Los Angeles, CA) (Van de Walle *et al.*, 2007). The vIL-8-Fc-His vector enabled construction of baculovirus expressing vIL-8 with a Fc-His tag, while the empty vector allowed construction of baculovirus expressing the Fc-His-only control protein. Furthermore the pFastBac11-Cpo-Fc-His-vIL-8 was used to generate pFastBac11-Cpo-Fc-His-vIL-8_ELR and pFastBac11-Cpo-Fc-His-vIL-8ΔCT with analogue mutations to the virus mutants described above by site directed mutagenesis. pFastBac11-Cpo-Fc-His-vIL-8 was amplified with primers containing the desired mutations (Table 1). The linearized plasmid was then electroporated into recombination competent GS1783 where re-circularisation of the plasmid occurred. Clones were screened with restriction enzymes and sequenced. All expression constructs were transferred into the baculovirus genome using TnR4 transposon mutagenesis as indicated in the manufacturer's instructions (Invitrogen) and positive clones were selected by blue-white screening.

2.5.2 Expression of recombinant vIL-8.

Recombinant bacmid DNA was purified by DNA mini-prep (2.2.1) and were transfected into SF9 insect cells to reconstitute the recombinant baculoviruses. Baculoviruses were propagated and titrated on SF9 cells. Expression of the recombinant vIL-8-Fc-His, vIL-8_ELR-Fc-His, vIL-8ΔC-term and Fc-His protein from the recombinant baculoviruses was confirmed by Western blotting. Recombinant vIL-8-Fc-His, vIL-8_ELR-Fc-His, vIL-8ΔC-term and Fc-His were purified by protein G affinity chromatography. Supernatant from infected SF9 cells was harvested 72 to 96 h post infection, diluted 1:2 with binding buffer and applied to a protein G column (Pierce). The column was washed with binding buffer, target proteins eluted with elution buffer, and neutralized with 1M Tris, pH 9 (Ausländer, 2007). Recombinant protein was analyzed by western blotting as described above, and purity determined by Coomassie brilliant blue staining. Fractions containing pure vIL-8-Fc-His, vIL-8_ELR-Fc-His, vIL-8ΔC-term or Fc-His were collected, protein concentrations determined using Bradford assay (Pierce), and aliquots stored at -80°C.

2.5.3 Isolation of Chicken PBMCs.

Chicken PBMCs were prepared from fresh chicken blood, kindly provided by the Institut für Geflügelkrankheiten of Freie Universität Berlin, and stored until processing in sodium citrate buffer to prevent coagulation. To isolate PBMCs, blood was mixed at a 1:1 ratio with PBS and overlayed on a Bicoll 1.077g/ml gradient (Biochrom). PBMCs were separated from erythrocytes and heterophils by centrifugation for 20 min 300×g, PBMC containing layer isolated and washed with PBS. To determine the concentration of cells, the pellet was then resuspended in 5 ml PBS 1% FCS. A small cell sample was mixed 1:1 with trypane blue and cells were counted using a modified Neubauer counting chamber.

2.5.4 Binding assay and flow cytometry

One million cells were washed with PBS 1 % FCS, incubated with 250nM vIL-8-Fc-His, vIL-8_ELR-Fc-His, or Fc-His and stained with mouse anti-Bu1, mouse-anti-chicken CD4 or anti-chicken CD8 antibodies (Southern Biotech), each at a 1:500 dilution. After washing with PBS, secondary anti-huFc-Cy5, anti-mouse-IgG AlexaFluor 488 (Fab fragment) and anti-mouse-IgM-FITC antibodies were used at dilutions of 1:1,000 followed again by washing with PBS 1 % FCS. CD25 staining was performed as the last step of the staining procedure using a PE-labeled mouse anti-CD25 antibody at a 1:100 dilution (Shanmugasundaram and Selvaraj, 2011). Stained cells were fixed with 0.5 % PFA, analyzed using the FACScalibur

flow cytometer (BD Bioscience) and data evaluated using the FlowJo software (Tree Star Inc.).

2.5.5 Chemotaxis assay.

Freshly isolated PBMCs were resuspended in chemotaxis media at a concentration of $1x10^6$ cells/ml. Chemotaxis assays were performed as described previously (Guinamard *et al.*, 1999) using transwell plates with 5 µm pore polycarbonate membranes (Corning Costar) according to the manufacturer's instructions. Briefly, vIL-8-huFc-His, huFc-His or 9E3/CEF4 were diluted to 50 nM in chemotaxis media and 600 µL added to the lower chamber. Fibronectin (5µg/ml) served as a positive control. $1x10^5$ PBMCs were added to the upper chamber and incubated for 40 min at 42°C. Migrated cells and input cells were measured for 30 s or 120 s at a constant flow rate by flow cytometry as described previously(Guinamard *et al.*, 1999).

2.5.6 Characterization of migrated cells.

To determine the cell populations that migrate in chemotaxis assays, 100 µl of the cells in the lower chamber were settled on polylysine slides for 3 hours in a wet chamber at 37°C, washed with PBS containing 1% FCS and fixed with 0.5% paraformaldehyde (PFA) at 4°C. Slides were stained with mouse anti-Bu1, -CD4, -CD8 or –CD25 antibodies at 1:500 dilutions, washed with PBS 1%FCS and visualized using Alexa Fluor 488 anti-mouse IgG antibodies (Invitrogen) at 1:1,000 dilutions. Slides were mounted with DAPI VectaShield (Vector Laboratories Inc.) and images taken with the Axiovert M1microscope system (Zeiss) and the number of B cells, CD4 or CD8 T cells determined for each sample using the AxioVision software (Zeiss).

2.6 Statistical analysis.

Statistical analysis was performed using the SPSS software (IBM) and StatXact (StatCon) for the Fisher-Freeman-Hamilton test. In general, data sets were first tested for normal distribution and depending on the result, the appropriate parametric or non-parametric test was chosen. Plaque size data of MDV recombinant viruses were analyzed using the Mann-Whitney-U test and one-way ANOVA. Data on MDV genome copies in whole blood samples were analyzed using Kruskal-Wallis and Mann-Whitney U tests. For analysis of the tumor incidence from the *in vivo* experiments, Fisher's exact and Fisher-Freeman-Hamilton tests were used. Results from chemotaxis and migration assays were analyzed by one-way ANOVA.

3 Results

3.1 Generation and characterization of vΔIR$_L$

Two copies of the *vIL-8* gene are present in the MDV genome, one in each R$_L$. To abrogate IL-8 expression both loci have to be mutated. However, targeting a locus in the R$_L$ often poses a technical challenge and requires the screening of numerous clones. To facilitate mutagenesis of *vIL-8* and in the future other genes in this region, we deleted most of the internal repeat long region (ΔIR$_L$) containing vIL-8 in pRB-1B (pΔIR$_L$, Fig. 4B and 5C) (Tischer *et al.*, 2006a). To determine if this deletion had an effect on MDV replication and pathogenesis, we tested the mutant *in vitro* and *in vivo*. Multi-cycle growth kinetics and plaque size assays showed that vΔIR$_L$ replicates comparable to parental vRB-1B (Fig. 5A and B). Furthermore, vΔIR$_L$ induced disease and lymphomas *in vivo* at rates comparable to the parental vRB-1B (data not shown). To determine if the deletion was restored upon reconstitution of the virus, I isolated DNA from infected cells and from tumor cell samples and analyzed them by PCR. Specific primers upstream and downstream of the deletion site allowed me to address restoration of the deletion site. Virus or BAC DNA containing the deletion resulted in a PCR amplicon of about 500bp, which served as a positive control indicating that the deletion is present. Restoration in the reconstituted virus would result in a 10kb amplicon, which was not generated under the PCR conditions used in this experiment. To show that viral DNA was indeed isolated from infected cells, I used a PCR amplifying vIL-8 as a control. Here I could demonstrate that the IR$_L$ deletion is already repaired in passage II after transfection (Fig. 5D).

3.2 The role and function of vIL-8 during MD pathogenesis and tumorigenesis

3.2.1 Generation and *in vitro* characterization of vΔMetvIL-8

Previously, a recombinant MDV lacking the entire vIL-8 open reading frame (ORF) was shown to be unable to efficiently produce lymphomas in inoculated chickens (Parcells *et al.*, 2001). However, it remained unclear whether this defect was caused by the absence of the vIL-8 chemokine or of one or more of the splice variants that vIL-8 exons II and III form with Meq, ORF4, and ORF5a (Fig. 4A) (Jarosinski and Schat, 2007). To determine to what extent

the secreted vIL-8 contributes to MDV pathogenesis, I introduced a point mutation in the vIL-8 start codon to abrogate its expression without affecting splicing with other genes. To address this question, I mutated the vIL-8 start codon (pΔMetvIL-8) in the remaining R_L copy of pΔIR_L, to determine the role of the secreted chemokine (Fig. 4B). Reconstitution of pΔMetvIL-8 resulted in viable virus (vΔMetvIL-8) that replicated in a fashion that was comparable to that of parental and revertant viruses (vΔMetvIL-8rev), as evidenced in multi-cycle growth kinetics and plaque size assays *in vitro* (Fig. 6A and B). To confirm that the vIL-8 start codon mutation indeed resulted in loss of vIL-8 expression and secretion, we performed western blot analysis to detect the vIL-8 protein in cell culture supernatant of infected CEC (Fig. 6C). Supernatants from vΔMetvIL-8 infected cells did not contain vIL-8, while the chemokine was readily detectable in cells infected with parental or revertant virus. In addition, I was able to amplify spliced vIL-8 transcripts, i.e. for vIL-8 chemokine and Meq-vIL-8, from cDNA, indicating that the point mutation of the vIL-8 start codon does not interfere with splicing in the Meq-vIL-8 region (Fig. 6D).

3.2.2 The secreted chemokine vIL-8 plays a role in MDV pathogenesis

3.2.2.1 vΔMetvIL-8 is impaired in MD pathogenesis and tumor formation

To elucidate if secreted vIL-8 is involved in MDV pathogenesis and lymphomagenesis, I infected 1- or 2-day old Valo chickens with vΔIR_L, vΔMetvIL-8, or vΔMetvIL-8rev and monitored them for 63 days or 91 days in two independent experiments. To analyze MDV lytic replication, I performed qPCR analysis on DNA from whole blood of infected chickens. MDV genome copies of vΔMet-vIL-8 were slightly reduced compared to those observed after infection with parental and revertant viruses (Fig. 7A and B). Furthermore, I monitored disease development over the course of the experiments. Only 46% (Exp-1) and 42% (Exp-2) of the chickens infected with vΔMet-vIL-8 developed MD, while 92% (ΔIRL), and 100% (ΔMetvIL-8rev) succumbed to disease at termination of the experiments, indicating that secreted vIL-8 contributes to MDV pathogenesis (Fig. 7C and D). Total tumor incidence after final necropsies was also reduced to 70% and 42% in Exp-1 and Exp-2, respectively (Fig. 7E and F). To determine if a reversion of the start codon mutation in vΔMetvIL-8 was responsible for the residual lymphomagenesis in infected animals, I isolated DNA from tumor cells and sequenced the vIL-8 region. Sequence analysis confirmed that the start codon mutation was present in all vΔMetvIL-8 induced tumors (data not shown), indicating that the mutation was stable *in vivo.* Taken together, my data demonstrated that abrogation of vIL-8 expression severely attenuates viral pathogenesis and lymphomagenesis in MDV.

3.2.2.2 vΔMetvIL-8 is severely impaired for the establishment of infection in contact chickens.

To determine if vIL-8 is involved in the establishment of MDV infection via the natural route of infection, we housed naïve chickens with vΔMetvIL-8 or vΔMetvIL-8rev infected animals in the second experiment. Even though vΔMetvIL-8 was able to spread to naïve chickens, MDV genome copies were only detectable at low levels in the blood of only a few vΔMetvIL-8 contact animals. In virus-positive chickens, MDV loads in the blood were decreased by more than 1,000-fold in vΔMetvIL-8 contact chickens when compared to animals infected with revertant virus (Fig. 8A). Furthermore, viral loads in the blood of vΔMetvIL-8 contact chickens only slightly increased over time, suggesting that the establishment of MDV infection is severely impaired in the absence of the secreted vIL-8 chemokine. To confirm these findings, we monitored disease incidence over the course of the experiment. None of the ΔMetvIL-8 contact chickens developed disease over the 91 days of the experiment and only one chicken had minor pathological lesions in the testes, while the revertant virus induced severe disease in most of the contact animals (Fig. 8B). Taken together, our data demonstrated that the secreted chemokine is essential for the establishment of MD via the natural route.

3.2.3 Functional mechanism of vIL-8

3.2.3.1 vIL-8 binds to and attracts B cells

Parcells and colleagues previously reported that vIL-8 attracts a fraction of chicken PBMCs, but did not identify the concerned PBMC subset (Parcells *et al.*, 2001). To elucidate precisely which cell populations are recruited by vIL-8, we expressed recombinant vIL-8-Fc-His using a baculovirus expression system, and performed *in vitro* binding and chemotaxis assays. Binding assays revealed that vIL-8-Fc-His, but not the Fc-His control protein (Fig. 9B, left panel), bound to B cells, which represent the main target of MDV lytic replication (Calnek, 2001). Besides B cells, vIL-8-Fc-His also interacted with about 10% of $CD4^+$ T cells, but not with $CD8^+$ T cells (Fig. 9B, middle and right panels). To test if vIL-8 could also induce cell migration, we performed chemotaxis assays with chicken PBMC. vIL-8-Fc-His efficiently induced chemotaxis of PBMC resulting on average in a 3-4 fold increase in migration when compared to the Fc-His control protein or 9E3/CEF4, a chemokine that mainly attracts monocytes and macrophages (Fig. 9C) (Calnek, 1986). To determine the PBMC subset that migrated in the presence of vIL-8-Fc-His, we fixed migrated cells on polylysine slides and stained for B cell as well as $CD4^+$ and $CD8^+$ T cell markers. The

percentage of B cells was significantly increased in the presence of vIL-8, while B cell ratios were not altered using the Fc-His control protein when compared to the input control (Fig. 9D). In contrast, we did not observe a significant difference in the percentage of $CD4^+$ or $CD8^+$ T cells in the presence of vIL-8-huFc-His. Our data demonstrated that vIL-8 is able to bind to and recruit B cells, suggesting vIL-8 expression of infected cells *in vivo* could aid the recruitment of B cells to the site of infection.

3.2.3.2 vIL-8 interacts with CD4+CD25+ T cells

In our binding assays (Fig. 9B) we observed that a small subset of $CD4^+$ T cells bound to vIL-8-Fc-His. Since $CD4^+$ T cells are the target for latent MDV infection and transformation, we decided to further characterize this population. As MDV tumor cells have been previously shown to mainly consist of $CD25^+$ regulatory T cells (Shanmugasundaram and Selvaraj, 2011), we determined if $CD4^+CD25^+$ T cells can bind vIL-8-Fc-His. Strikingly, all $CD25^+$ cells were able to bind vIL-8-Fc-His (Fig. 10A). Furthermore, we could demonstrate that vIL-8-Fc-His strongly labeled $CD4^+CD25^+$ T cells to the point that virtually all of these cells appeared to bind vIL-8-Fc-His in our assays (Fig. 10B), suggesting that these cells could be recruited to the site of infection *in vivo* by secreted vIL-8.

3.2.3.3 CD25 is differentially expressed on ex vivo tumor cells from vΔMetvIL-8 infected animals.

In order to address if absence of vIL-8 expression in MDV infected chickens affects recruitment of target cells for transformation and therefore the phenotype of tumor cells, I investigated the expression of the activation marker CD25 on the surface of ex vivo tumor cells derived from chickens infected with vΔMetvIL-8, parental or revertant virus (Fig. 11). Intriguingly, I could observe only very low CD25 expression levels in one out of two vΔMetvIL-8 tumor cells, while all parental or revertant virus tumor cells expressed high levels of CD25. Further studies will be needed to determine if vΔMetvIL-8 tumor cells have a different phenotype than wild type MDV tumor cells.

3.3 Generation of vIL-8 mutants targeting functional motifs of vIL-8

3.3.1 Generation and *in vitro* characterization of vIL-8_ELR and ΔCT-vIL-8

Previous studies revelaed that PBMC are the target for vIL-8 in chemotaxis assays (Parcells *et al.*, 2001)). Cellular IL-8 contains a three amino acid motif ELR preceding the CXC box that determines receptor specificity. To investigate whether the DKR motif

determines specificity of vIL-8 for B cells I constructed pvIL-8_ELR with a substitution of DKR by ELR (Fig. 4B). Furthermore, it was proposed that vIL-8 could enhance neovascularisation in tumors (Cui *et al.*, 2004; Parcells *et al.*, 2001). Studies on other CXC chemokines have suggested a role for the C-terminus in angiogenesis that may be either angiogenic or angiostatic (Maione *et al.*, 1990; Sharpe *et al.*, 1990; Strieter *et al.*, 1995). Therefore, I generated pvIL-8ΔCT which contains a premature stop codon inserted within the C-terminus of vIL-8 (Fig. 4B). Multi-step growth kinetics and plaque size analysis showed that both mutants and their revertants replicated comparable to parental virus (Fig. 12A and B), indicating that neither substitution of DKR by ELR nor the shorter C-terminus affect replication of the virus *in vitro*.

3.3.2 vIL-8_ELR shares binding properties of vIL-8

To investigate if the ELR motif of vIL-8 changes the vIL-8 binding properties to B cells and $CD4^+$ T cells, I generated baculovirus expression constructs for vIL-8_ELR-huFc-His and vIL-8ΔC-term-huFc-His based on the wt vIL-8-huFc-His as described above. The vIL-8_ELR-huFc-His was efficiently expressed in baculovirus infected SF9 cells and could be purified using Protein G column as described above. In contrast to vIL-8_ELR-huFc-His vIL-8ΔC-term-huFc-His could not be expressed although sequencing results confirmed the construct and multiple expression construct clones were tested for expression. Likely vIL-8ΔCT-huFc-His was instable or misfolded due to the truncation of the protein.

vIL-8_ELR-huFc-His efficiently bound to B cells and a small subset of $CD4^+$ T cells in a comparable fashion as vIL-8-huFc-His suggesting that the ELR motif is not responsible for receptor specificity as described for mammalian IL-8 (Fig. 13). Due to this result and a recent published study on the pathogenesis of a similar vIL-8_ELR mutant (Cui *et al.*, 2004), we decided to not further analyze our vIL-8_ELR mutant *in vivo*.

3.3.3 Characterization of vΔCT-vIL-8 *in vivo*

To investigate the role of the vIL-8C terminus in MDV pathogenesis, I infected 2-day old SPF Valo chickens with vΔCT-vIL-8 or vΔCT-vIL-8rev. As a wild type control, vΔMetvIL-8 rev from 3.2.2.2 was used as a wild type control as both experiments were run in parallel and I could show before that vΔMetvIL-8 rev causes disease similar to wild type virus. Chickens were monitored for 91 days. vΔCT-vIL-8 infection resulted in a MD incidence of 80%, while 100% of the animals infected with wild type virus developed disease, suggesting that the vIL-8 C-terminus has only a minor role in the function of vIL-8 (Fig 14A). After final necropsies, I found tumors in 80% of the vvIL-8ΔC-term infected chickens while the wild type virus

caused tumors in all infected chickens (Fig. 14C). Contact birds of vvIL-8ΔC-term and wild type virus groups developed MD in 30% and 60% of the animals respectively suggesting that vΔCT-vIL-8 is transmitted, but pathogenesis is reduced compared to wild type virus (Fig. 14B). Tumors in vΔCT-vIL-8 contact chickens were found in 40% of the animals while in wild type contact chickens 55% of the animals had tumors. (Fig. 14D).

However, the revertant virus (vΔCT-vIL-8 rev) caused MD to a significantly lower extent than wild type virus. Only 66% of the chickens infected with vΔCT-vIL-8 rev developed MD while tumors were found in 70% of the chickens at the end of the experiment (Fig. 14A). The fact, that MD incidence in the revertant group is similar to the vΔCT-vIL-8 group indicates that the revertant virus is likely to have acquired secondary mutations in other locations than the vIL-8 C-terminus resulting in a reduced pathogenesis *in vivo*. Therefore the results from this experiment remained inconclusive and need to be revisited in order to draw a conclusion on the role of the vIL-8 C-terminus in pathogenesis.

3.4 Generation of an indicator virus for lytic and latent phase of viral life cycle

3.4.1 Generation and characterization of a UL47-RFP_Meq-GFP markervirus

In a recent study, Jarosinski and colleagues (Jarosinski *et al.*, 2012) generated a recombinant virus harboring a red fluorescent protein (RFP) fused to the C-terminus of the UL47 tegument protein in the oncogenic RB-1B strain. This markervirus allowed identification of lytically infected cells *in vitro* and could shed light on the MDV life cycle *in vivo*. However, UL47-GFP is not expressed in latently infected cells. To overcome this obstacle, I generated a virus that had a green fluorescent protein fused to the C-terminus of the major MDV oncogene Meq that expressed at high levels during latency and in transformed cells (Fig. 15A). Upon insertion of the GFP, we deleted the IR_L as described in 3.1.

As Meq is expressed only at very low levels during lytic infection vUL47-RFP_Meq-GFP allows a distinction between lytically and latently infected cells *in vitro* and *in vivo*. Reconstitution of vUL47-RFP_Meq-GFP confirmed that Meq-GFP is expressed at very low levels lytically infected CECs while UL47-RFP was expressed at high levels *in vitro* (data not shown). Plaque size analysis confirmed that vUL47-RFP_Meq-GFP has no growth defect implicating that tagging of Meq with GFP does not inhibit viral replication (Fig. 15B).

3.4.2 *In vivo* characterization of vUL47-RFP_Meq-GFP markervirus

To track lytic and latently infected cells in cells *in vivo*, one day old Valo SPF chickens were infected with vUL47-RFP_Meq-GFP. Infected chickens were co-housed with contact

animals to determine if the virus was able to spread to naïve animals. Infected chickens were monitored for 13 weeks for clinical signs of MD. Intriguingly, neither infected nor contact animals developed MD symptoms (Fig. 15C), indicating that insertion of GFP at the C-terminus of Meq has an effect on MDV pathogenesis.

4 Discussion

The aims of my thesis were (1) to generate a tool facilitating mutagenesis of the genes located in the repeats long; (2) to determine the role of the secreted chemokine vIL-8 in the pathogenesis and tumorigenesis of MD and to define the mechanism by which vIL-8 is able to influence pathogenesis and tumorigenesis of MD; (3) to investigate the impact of the DKR motif and the C-terminus of vIL-8 on vIL-8 function;; and (4) to develop a markervirus for lytic and latent infection.

4.1 Generation of a tool for mutagenesis in the repeats long region

In order to generate a tool facilitating the mutation of diploid genes located in the repeats long, I deleted most of the IR_L in pRB-1B ($v\Delta IR_L$), leaving only terminal sequences of ~0.5 kb and ~1.5 kb of the IR_L. $v\Delta IR_L$ replicated and induced disease with an efficiency that was comparable to the parental virus. More importantly, the deleted IR_L sequences were completely restored within two passages post reconstitution. The mutations introduced into the TR_L were thereby copied into the IR_L locus.

Replication of HSV, the alphaherpesvirus prototype, is associated with a high frequency of intra- and intergenomic recombination (Bataille and Epstein, 1995; Roizman, 1979). In addition, a strong selection for the presence of essential genes located in the R_L which could possibly enhance restoration of the IR_L during virus replication. In case of $v\Delta IR_L$, restoration of the deleted sequences appears to be highly favorable as the deletion is already repaired upon two passages *in vitro*. Thus the mutant is an appropriate platform for rapid manipulation of genes located in the R_L region facilitating the analysis of these genes in the viral background. Furthermore, the viability and pathogenicity of $v\Delta IR_L$ suggests, that one intact repeat long is sufficient to reconstitute MDV. Therefore, a similar strategy to delete one of the R_S could be tested and evaluated as a platform for a rapid manipulation of genes in the R_S.

4.2 Idenfication of the role and function of vIL-8 in MD pathogenesis

My second aim was to investigate the role of the secreted vIL-8 chemokine in MDV pathogenesis. Furthermore, I studied how this viral chemokine can modulate the immune system to aid in the establishment of MDV infection and lymphomagenesis. Previously, it was reported that deletion of the entire vIL-8 ORF in the MDV genome resulted in viruses that were severely impaired with respect to lymphomagenesis and disease induction (Cui *et al.*,

2004; Parcells *et al.*, 2001). Moreover, a vIL-8 deletion mutant efficiently replicated in feather follicle epithelium, spread to naïve animals and induced high antibody titers in contact chickens (Cui *et al.*, 2004). Intriguingly, Jarosinski and Schat discovered that the vIL-8 exon II and III are not only part of the secreted chemokine, but also part of a spliced "fusion protein" that also include the upstream genes *meq, ORF4* and/or *ORF5a* (Fig. 4A) (Jarosinski and Schat, 2007). The data raised the question to what extent the secreted vIL-8 chemokine or the splice variants contribute to the observed phenotype of vIL-8 deletion viruses. Anobile and colleagues reported that Meq-vIL-8 localizes to the nucleoplasm, nucleoli and Cajal bodies (Anobile *et al.*, 2006). Moreover, Meq-vIL-8 is able to form homodimers, and shows distinct mobility patterns that differ compared to those of Meq, suggesting that the splice variants may indeed have a biological relevance (Anobile *et al.*, 2006). Furthermore, an exon I deletion mutant was previously generated to determine the role of the secreted vIL-8 chemokine by itself. This mutant virus exhibited a defect in lytic replication when chickens were infected at the age of two days *in vivo* and resulted in an MD incidence of only about 40%, suggesting that vIL-8 contributes to MDV pathogenesis, but not to such a striking degree as was seen in the complete vIL-8 deletion mutants (Jarosinski and Schat, 2007). However, *in silico* predictions (Human Splicing Finder v. 2.4.1) (Hamroun *et al.*, 2010) indicated that a branch point and three potential splice acceptor sites with high consensus values are present in exon I of vIL-8. Therefore, in this study I generated a mutant, vΔMetvIL-8, that does not interfere with splicing in the region. I observed that vΔMetvIL-8 has a reduced disease and lymphoma incidence when compared to wild-type and revertant virus. However, vΔMetvIL-8 is more pathogenic than complete vIL-8 deletion mutants, which induce tumors in only ~10 % of the chickens (Parcells *et al.*, 2001). Taken together, our data and data from other groups confirm that vIL-8 plays an important role in MD pathogenesis, but that the previously published vIL-8 deletion mutant likely exhibited a "composite phenotype," perhaps due to effects on the transcriptional program and/or splice variants, and not solely due to a lack of vIL-8 expression. Further studies will be needed to determine if and to what extent the various vIL-8 splice variants or potential regulatory sequences contribute to the pathogenesis of MDV. Moreover, Parcells and coworkers hypothesized that vIL-8 might recruit target cells to facilitate viral spread, a process that likely plays an important role during the early stages of infection (Cui *et al.*, 2004; Jarosinski and Schat, 2007; Parcells *et al.*, 2001). I was able to detect vΔMetvIL-8 in contact chickens, but only at very low levels. My results therefore suggest that vIL-8 is important for the establishment of infection, or for efficient spread or shedding of infectious virus.

Previously, vIL-8 had already been shown to induce chemotaxis of an unidentified subpopulation of PBMCs, suggesting that MDV might recruit specific cell types to the site of infection, which could play important roles in viral pathogenesis. Sequence alignment of vIL-8 with other chemokines revealed a homology to the B-lymphocyte chemo attractant, or chicken CXCL13 family members (Gunn *et al.*, 1998; Kaiser *et al.*, 2005). Strikingly, vIL-8 bound and induced migration of B cells, the main target of MDV lytic replication (Calnek *et al.*, 1984). MDV-infected B- cells can be detected as early as 2 days after inhalation of the virus in the lung (Baaten *et al.*, 2009). Thus, it is tempting to speculate that the vIL-8 chemokine might recruit B cells to the initial site of infection in the lung. Furthermore, the well-known delay in disease progression in the absence of B cells, e.g. upon bursectomy, underscores that B cells play a central role during early infection (Baaten *et al.*, 2009; Schat *et al.*, 1981). The lack of B cell recruitment in vΔMetvIL-8 infected chickens could explain the reduced viral load in chickens infected via the natural route and thus the lack of disease progression in these birds. Reduced levels of infected B cells in the absence of vIL-8 might, therefore, result in a less efficient infection of $CD4^+$ T- cells, and as such, decrease the likelihood of T cell transformation and lymphomagenesis.

Previous studies demonstrated that primary MDV tumor cells have a T_{reg} phenotype, as transformed cells were shown to express a number of well-established markers for regulatory cells such as CD4 and CD25 (Burgess and Davison, 2002; Shack *et al.*, 2008). In this study, I was able to demonstrate that vIL-8 specifically binds to $CD4^+CD25^+$ T cells, which suggests that vIL-8 might recruit these activated cells as a target for infection and transformation. As CD25 is a component of the IL-2 receptor (IL-2R), which promotes cell proliferation and increased viability of naïve T cells, it is possible that IL-2R signaling is subverted in the initial stages of transformation and immortalization resulting in lymphomagenesis (Burgess and Davison, 2002). From immunological studies in mice and human it is well known that a subset of T cells, the so called follicular B helper cells (T_{FH}), expresses CXCR5 and binds and responds to CXCL13 (Cyster *et al.*, 2000). Activated T cells upregulate CXCR5 upon CXCL13 stimulus and home to follicles where they establish close contact with B cells (Ansel *et al.*, 1999). Therefore T_{FH} cells in chickens might be a recruited to MDV infected B cells, a hypothesis that could be addressed in future studies. Alternatively, it is tempting to speculate that the recruited $CD4^+CD25^+$ T cells have or acquire a regulatory phenotype that might suppress anti-tumor immune responses.

Intriguingly, tumor cells derived from vΔMetvIL-8 may vary in their phenotype from cells transformed with parental or revertant virus. CD25 expression was not present in two out of

three tumor samples derived from two different chickens infected with vΔMetvIL-8, suggesting that absence of the IL-8 chemokine might alter the cell types that are available to MDV for transformation such as activated $CD4^+CD25^+$ T cells. Schat and others have reported that the phenotype of MDV transformed cells is dependent on the availability of certain cell populations. Under natural conditions the phenotype of MDV transformed cells was shown to be rather uniform (Burgess and Davison, 2002; Calnek *et al.*, 1989; Calnek *et al.*, 1984; Schat *et al.*, 1981; Shack *et al.*, 2008; Shek *et al.*, 1983). However, further studies on a larger number of tumor samples are needed to confirm my observation and in order support the claim that vIL-8 elicits targeted recruitment of cell populations which are subsequently transformed. Nevertheless, binding of vIL-8 and the low CD25 expression on some tumor cell samples in the absence of vIL-8 provide the first evidence that MDV might actively recruit target cells for transformation (see Fig. 16 for model of vIL-8 function).

4.3 The impact of the vIL-8 DKR motif on its tropism and the function of vIL-8 C-terminus

The 3rd aim was to investigate the role of the DKR motif in vIL-8 and if this motif confers the specificity for binding to B cells. Therefore I generated a mutant harboring an ELR motif instead of DKR, to investigate whether replacement of DKR by ELR would alter the tropism of vIL-8. This mutant replicated comparable to the parental virus *in vitro*.

Intriguingly, the capacity of vIL-8 to bind to B cells and a subset of $CD4^+$ T cells was not altered by mutating the DKR motif to ELR. Furthermore, recent results on the pathogenesis of an ELR mutant virus demonstrated that a substitution of DKR by ELR does not affect pathogenesis, supporting the hypothesis that vIL-8 is not a true orthologue of IL-8 as proposed by Parcells and colleagues (Cui *et al.*, 2004; Parcells *et al.*, 2001). Instead these data support the *in silico* prediction data that vIL-8 is closely related to B cell homing chemokines, such as CXCL13Li1, CXCL13Li2 and CXCL13Li3 of the chicken (Kaiser *et al.*, 2005; Staeheli *et al.*, 2001). Based on our data, vCXCL13 would be a more appropriate term for the MDV chemokine than vIL-8 and would avoid confusion in terms of chemokine function.

Since it was previously proposed that the C-terminus of CXC chemokines either confers angiogenic or angiostatic properties in neovascularization of tumors, I hypothesized that the C-terminus could have important functions specific for MDV (Maione *et al.*, 1990; Sharpe *et al.*, 1990; Strieter *et al.*, 1995). Therefore I generated a vΔCT-vIL-8 and could demonstrate that it replicates comparable to parental virus and revertant (vΔCT-vIL-8 rev) *in vitro.* To investigate the effect of the C-terminal deletion on pathogenesis and tumorigenesis, I infected

Valo SPF chickens with this mutant and the revertant virus. Furthermore, naïve contact animals were co-housed to address questions concerning transmission of vvIL-8ΔC-term. vΔCT-vIL-8 infected animals developed MD and tumors almost to the same extent as animals in the wild type virus group suggesting that the vIL-8 C-terminus only plays a minor role for the function of vIL-8. However, the respective revertant appeared to be less efficient in inducing MD and tumors suggesting that the revertant has additional mutations that interfere with pathogenesis. Thus the data of this experiment remains to be confirmed using an intact revertant virus to confirm the phenotype and to ensure that the phenotype is indeed attributable to the deletion of the C-terminus of vIL-8. Furthermore, the mild reduction in pathogenesis and tumorigenesis of vvIL-8ΔC-term could be either a consequence of secreted vIL-8 chemokine function or splice variant function impairment.

4.4 Generation and characterization of a markervirus for lytic and latent infection *in vivo*

Jarosinski et al (Jarosinski *et al.*, 2012) previously described a UL47-GFP markervirus for lytic replication of MDV. This virus was detectable in various tissues *in vivo* expressing UL47-GFP at moderate levels, with the exception of feather follicle epithelium, where UL47-GFP was abundantly expressed. Characterization of this virus however only visualizes lytically infected cells. Therefore the aim was to generate a markervirus that allows differentiation of lytically and latently infected cells by tagging UL47 for lytic and Meq for latent infection with two different fluorescent proteins. This virus would aid to shed light on the different stages of the MDV life cycle *in vivo*. A virus resulting in fluorescently labeled latently infected tumor cells could help to characterize, track and locate those tumor cells in infected chicken and could shed further light on MDV pathogenesis and tumorigenesis.

Although vUL47-RFP_Meq-GFP replicated comparable to parental viruses *in vitro* and Meq-GFP was expressed, it was completely apathogenic *in vivo*. As Meq is the major oncogene in MDV, one likely explanation is that GFP interferes with the function of Meq as a transactivator to induce tumor formation in infected birds. Alternatively, it is conceivable, that GFP presented as a foreign antigen in latently infected and/or transformed cells increases the exposure of these cells to the immune system. Although vUL47-RFP_Meq-GFP cannot be used as a markervirus that causes cancer, this apathogenic virus may be used to characterize latently infected cells in the absence of transformation and tumor formation. All in all, other strategies need to be explored to generate an oncogenic markervirus that allows discrimination between lytic and latently infected cells in an oncogenic context.

5 Conclusions and summary

In conclusion, I successfully generated vΔIR_L, a novel tool for manipulation of important viral genes such as Meq, vIL-8 or vTR. Furthermore I demonstrated that the secreted vIL-8 chemokine plays an important role in MVD pathogenesis. My data suggest that vIL-8 is involved in various stages of pathogenesis from the establishment of infection to the development of tumors. I identified two novel target cells for vIL-8: B cells, which are the main substrate for lytic replication of MDV, and $CD4^+CD25^+$ T cells, a putative target for MDV transformation. My data also indicate that the DKR motif in vIL-8 can be exchanged with ELR without affecting the specificity of vIL-8 to its target cells, supporting the hypothesis that vIL-8 rather a CXCL13 orthologue. Moreover, the vIL-8 C-terminus does not appear to have a major role for the function of vIL-8 as it does not significantly affect MD pathogenesis.

In order to generate a markervirus for lytic and latent infection in an oncogenic background to study pathogenesis and tumorigenesis, vUL47-RFP_Meq-GFP was constructed and characterized *in vitro* and *in vivo*. Virus replication was not impaired *in vitro*, however this markervirus was completely attenuated *in vivo.* Although vUL47-RFP_Meq-GFP did not meet the expectations of an oncogenic markervirus, it is a suitable candidate to facilitate studying latency in the absence of transformation.

Tables

TABLE 1 Primers used for construction of virus mutants

construct	sequence (5‘-3‘)	direction
ΔR_L	GTATGTGTGGGAGAAAGTATGTCGATTTTAAATGTAGTT GGTCCTGTATCTACCTATAGGTAGGGATAACAGGGTAA TCGATTT	forward
	CCAATAACTCGAACGCTCTTCCTATAGGTAGATACAGG ACCAACTACATTTAAAATCGACGCCAGTGTTACAACCA ATTAACC	reverse
IR_L deletion	CGAACGGAATGTACAACAGCTTGC	forward sequencing
	GATAAGACACTTTCCCACTCATAC	reverse sequencing
ΔMetvIL-8	GCAGGGGGTGTGGGTTTGATGAGCAGTTGGGGCGGCAA AA**T**TGCAGGCGTTGTTGCTAGTATTGGTAGGGATAACA GGGTAATCGATTT	forward
	CAAATAGATCTGTACTATGAATAGAACCAATACTAGCA ACAACGCCTGCA**A**TTTTGCCGCCCCAACTGCTCATCGCC AGTGTTACAACCAATTAACC	reverse
ΔMetvIL-8rev	TGTACTATGAATAGAACCAATACTAGCAACAACGCCTG CA**T**TTTTGCCGCCCCAACTGCTAGTGTTACAACCAATTA ACC	forward
	GCAGGGGGTGTGGGTTTGATGAGCAGTTGGGGCGGCAA AA**A**TGCAGGCGTTGTTGCTAGTGATAACAGGGTAATCG ATTT	reverse
vIL-8 seq	CTGCTATGCAGGGGTCGTGGGAA	forward sequencing
	GCACCTCTTGTCGACAGCGAGAC	reverse sequencing
vIL-8_ELR	CAAGCCAGTAGGCCGATTAGTGACTTTCACGCACTTGCA CCT**GAGCTCGAC**AGCGAGACTCTCCAGTAGGGATAACA GGGTAATCGATTT	forward
	CTCTTAATAATGTAGGCATATCACTGGAGAGTCTCGCT**G TCGAGCTC**AGGTGCAAGTGCGTGAAAGGCCAGTGTTAC AACCAATTAACC	reverse
vIL-8_ELR rev	TTAATAATGTAGGCATATCACTGGAGAGTCTCGCTGTCG A**CAAGAG**GTGCAAGTGCGTGAGTAGGGATAACAGGGT AATC	forward
	CCAGTAGGCCGATTAGTGACTTTCACGCACTTGCACCT**C TTGTC**GACAGCGAGACTCTCCAGTGTTACAACCAATTA ACC	reverse
vIL-8_ELR seq	CCGTATCCCTGCTCCATCCAATAGC	forward sequencing
	GGTCTCCAATATCACGTGTTGGTGG	reverse sequencing
ΔCT-vIL-8	ATGGTGGCAAATCGACCGTGGGACCGGTAAAAAACACA **TTATAAGAG**CCCACACCTCCTAGTAGGGATAACAGGGT AATC	forward
	AGACAGATATGGGAACCAATAGTAGGAGGTGTGGG**CTC TTATAA**TGTGTTTTTTACCGGGCCAGTGTTACAACCAAT TAA	reverse
ΔCT-vIL-8 rev	ATGGTGGCAAATCGACCGTGGGACCGGTAAAAAACACA **ATTGAG**CCCACACCTCCTACTAGTAGGGATAACAGGGT AATC	forward
	GACAGATATGGGAACCAATAGTAGGAGGTGTGGG**CTCA AT**TGTGTTTTTTACCGGTCCCAGCCAGTGTTACAACCAA TTA	reverse
ΔCT-vIL-8 seq	CCGTATCCCTGCTCCATCCAATAGC	forward sequencing
	GGTCTCCAATATCACGTGTTGGTGG	reverse sequencing
Meq-GFP	CAGTCTACGGTCTGGTGGTTTCCAGGTGACGGGAGACC	forward

	CATGGTGAGCAAGGGCGAGG GACGATGTGCTGCTGAGAGTCACAATGCGGATCATCAC TTGTACAGCTCGTCCATGCCG	reverse
Meq-GFP seq	CAAGCAAAAGGGGAAGAGAG	forward sequencing
	GCATTGTGTCCTGTTACCGAG	reverse sequencing

*mutated sequences are shown in bold letters

TABLE 2 animal experiments

experiment	**virus**	**nr. of animals***	**nr. of contacts***
Exp-1	pΔIR_L	13 (1)	--
	pΔMetvIL-8	14 (1)	--
	pΔMetvIL-8 rev	13 (0)	--
Epx-2	pΔMetvIL-8	15 (1)	10 (1)
	pΔMetvIL-8 rev	15 (0)	10 (0)
	pΔCT-vIL-8	15 (0)	10 (0)
	pΔCT-vIL-8 rev	15 (0)	10 (0)
	pUL47-RFP_Meq-GFP	10 (0)	--

* number in brackets indicates number of animals excluded from the study

Figures

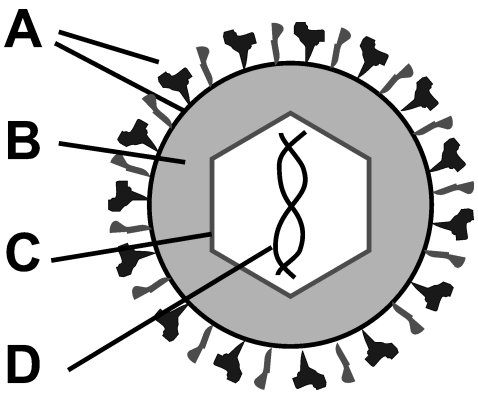

Figure 1: Schematic presentation of a herpesvirus virion. A. Lipid envelope with viral glycoproteins **B.** Tegument. **C.** Icosahedral capsid. **D.** Linear double-stranded DNA

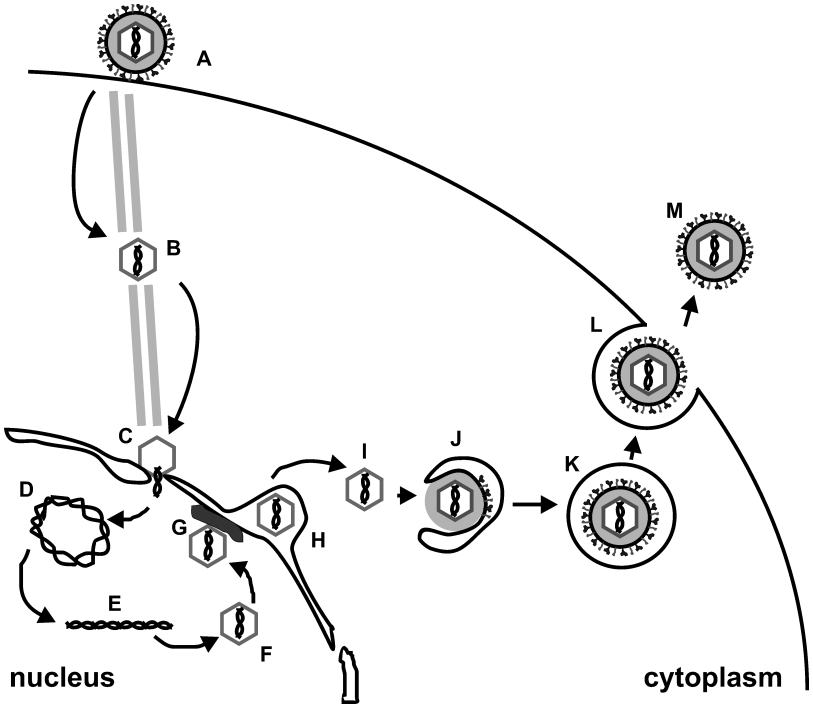

Figure 2: Schematic presentation of the alpha-herpesvirus life cycle (Mettenleiter *et al.*, 2006). The virion attaches to the cell surface and releases the capsid into the host cell (**A**). In the host cell, the capsid is transported along microtubules to the nucleus (**B**) where it docks to the nuclear pore and releases the DNA into the nucleus (**C**). Upon circularization (**D**), viral DNA is replicated as concatamers (**E**) which are subsequently cleaved into unit-length genomes and packaged into pre-assembled capsids (**F**). At the nuclear membrane, the capsids aquire a primary tegument (**G**) and bud at the inner lamina of the nuclear membrane (**H**). By fusion with the outer leaflet of the nuclear membrane the capsid is released into the cytoplasm (**I**). Maturation of the virion occurs at the trans-golgi networks via tegumentation and envelopment (**J** and **K**). Virus-containing vesicles reach the cell surface where mature virions are released from the cell (**L**).

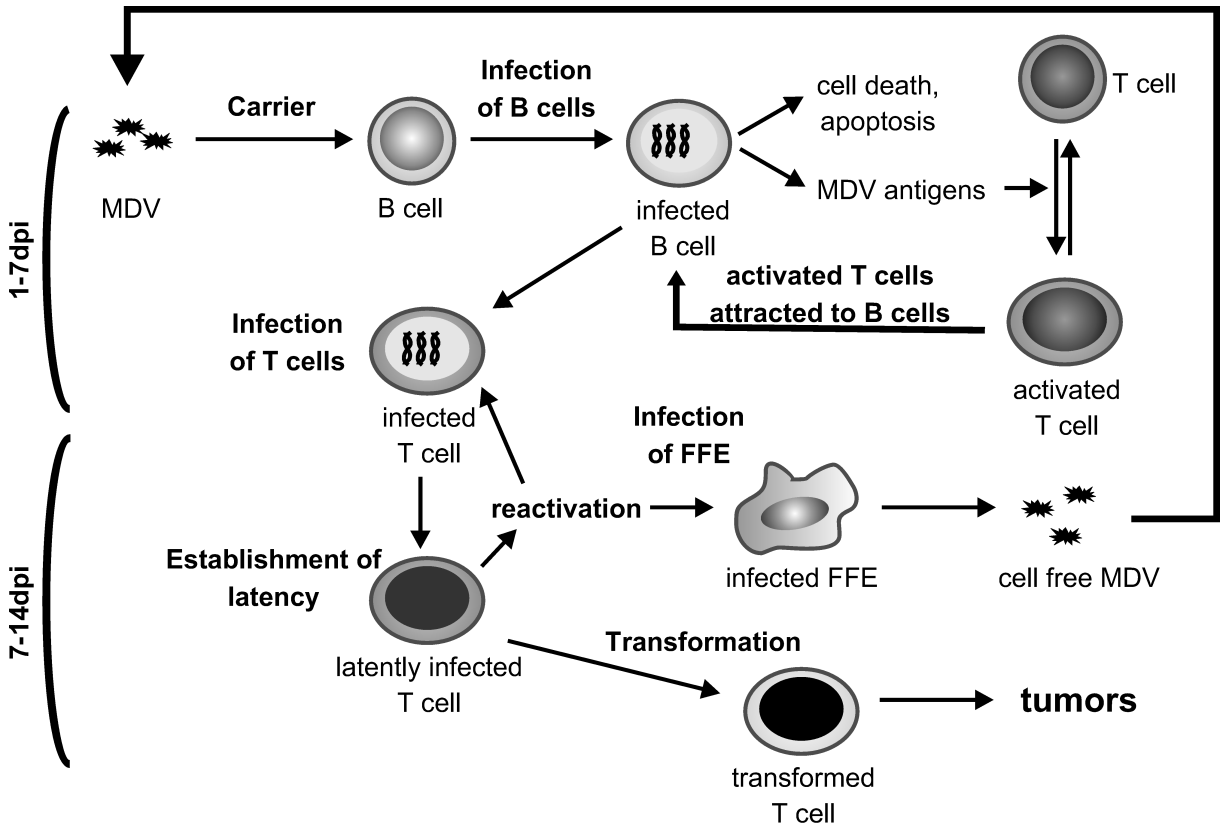

Figure 3: Model of MDV life cycle. Dander containing MDV is inhaled and reaches the lung where MDV is carried by macrophages and dendritic cells to lymphoid tissues where B cells are infected. Infected B cells undergo apoptosis, but also present viral antigens to activated T cells which in turn become infected. Infected T cells carry the virus to the feather follicle epithelium, where MDV productive infection and shedding of into the environment occurs. In addition, MDV establishes latency in T cells, which also serve as targets for transformation leading to tumor formation.

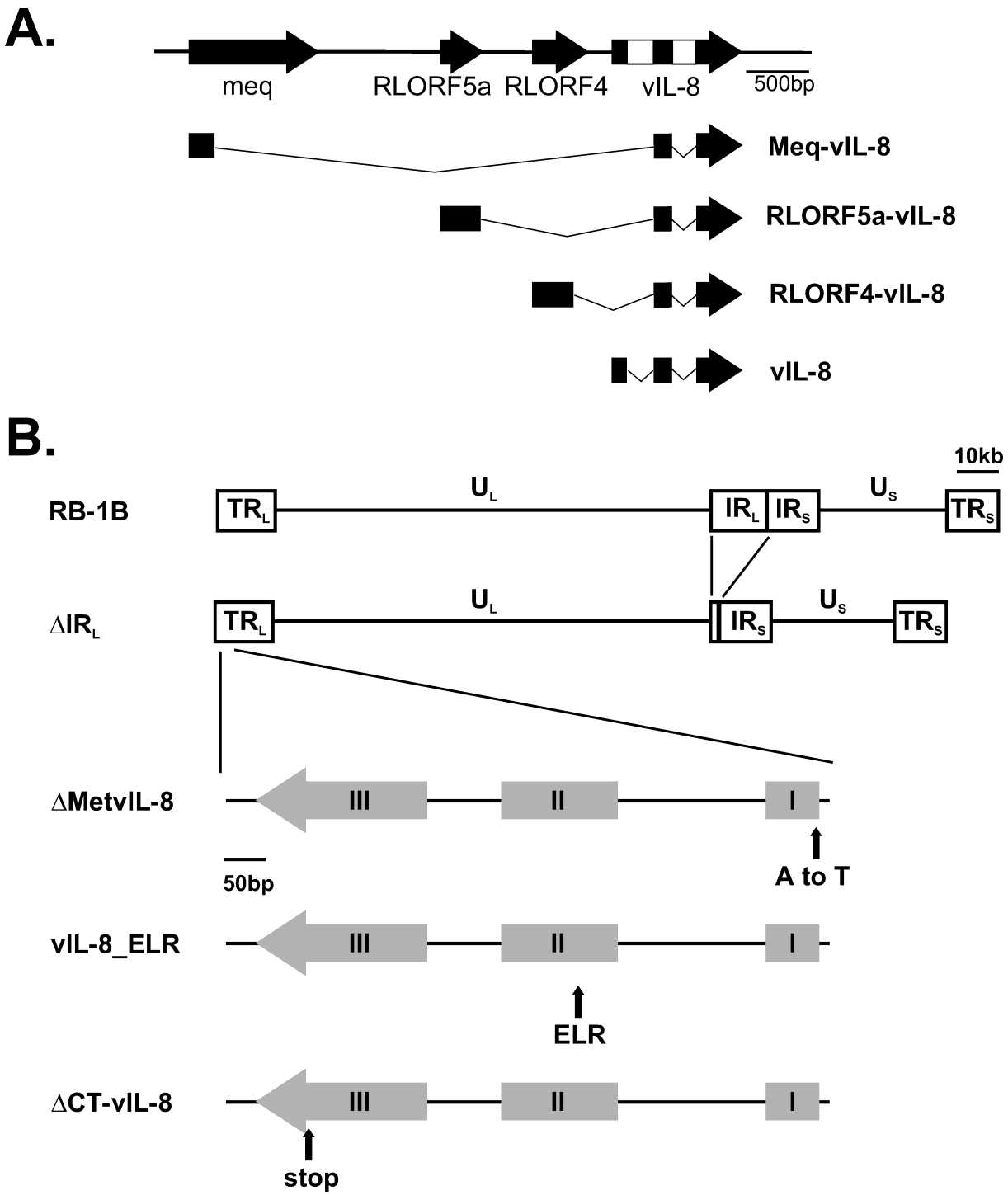

Figure 4: Overview of MDV genome and vIL-8 splice variants. A. Schematic representation of the repeat long region (R_L) region segment containing meq, RLORF4, RLORF5a and vIL-8. Splice variant of indicated genes with vIL-8 exon 2 and 3 are shown as described *in vitro* and/or *in vivo* by Jarosinski et al (Jarosinski and Schat, 2007). **B.** Overview of the MDV pRB-1B genome consisting of two unique regions, long (U_L) and short (U_S), flanked by terminal and internal repeats long (TR_L and IR_L) and short (TR_S and IR_S), respectively. Recombinant pRB-1B with a deletion of most of the IR_L (pΔ IR_L) and vIL-8 start codon mutation (pΔMetvIL-8), ELR motif (pvIL-8_ELR) and C-terminal deletion (pΔCT-vIL-8) in the TR_L are shown. **C.** Mutagenesis strategy for generating vΔIR_L UL47-RFP Meq-GFP.

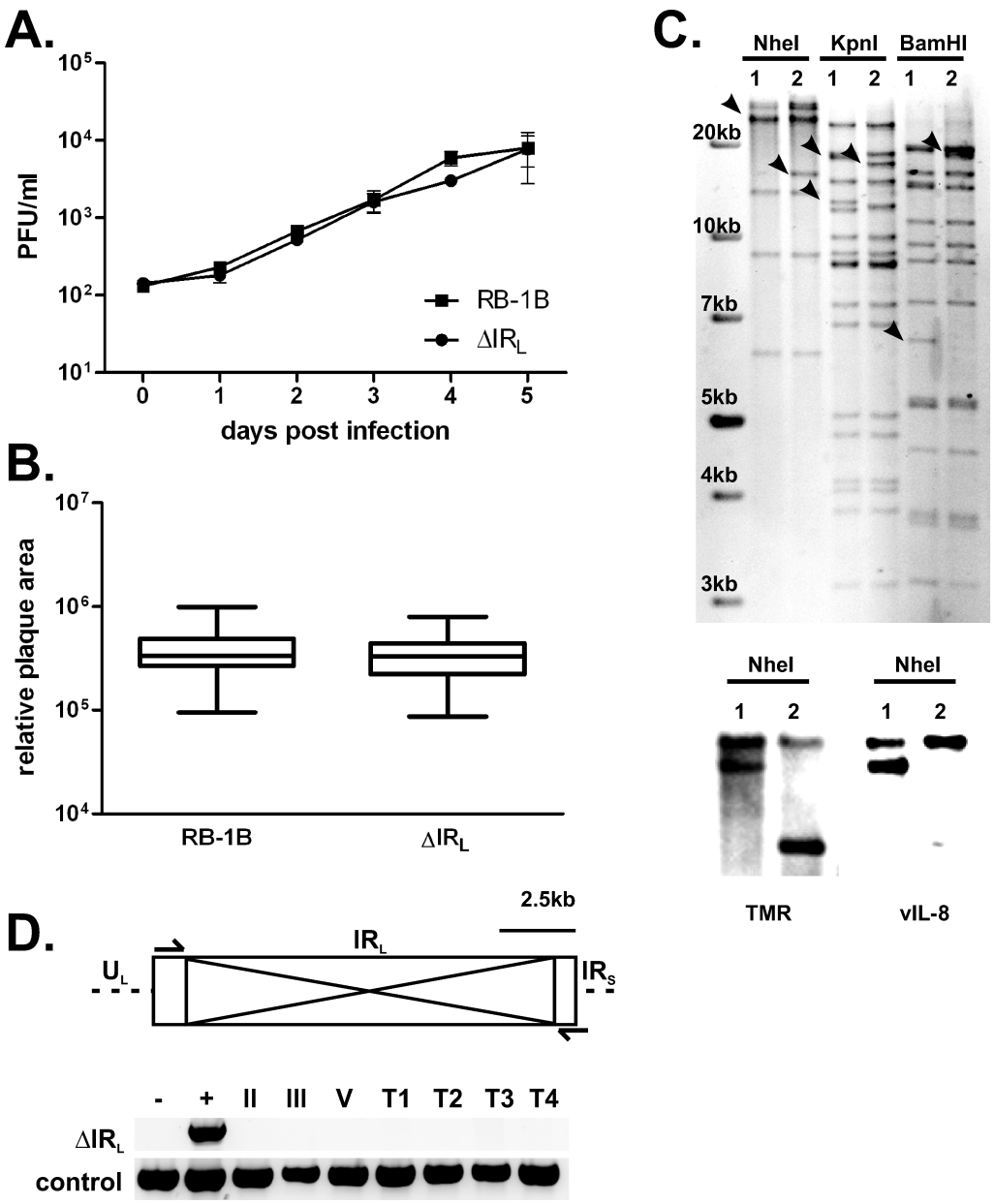

Figure 5: Characterization of vΔIR$_L$. A. Multi-step growth kinetics of recombinant viruses vRB-1B and vΔIR$_L$. **B.** Plaque area analysis of vRB-1B and vΔIR$_L$ (n=150 Mann-Whitney-U p>0.05;) Plaque sizes are shown as boxplots with minimum and maximum. **C.** RFLP and Southern blot analysis of pRB-1B (1) and pΔIR$_L$(2) with indicated restriction enzymes. Expected changes are indicated by arrows. Southern blot of an NheI digest of pRB-1B (1) and pΔIR$_L$(2). Fragments containing the R$_L$ were detected with digoxigenin-labeled probe specific for vIL-8 or the viral telomeric repeats present in the R$_L$ adjacent to the deletion. **D.** Restoration of the IR$_L$ in vΔIR$_L$ infected cells *in vitro* and *in vivo*. Schematic representation of the IR$_L$ in the MDV genome. Deleted sequences and primers used for the analysis are indicated. Deletion site was amplifies was from DNA extracted from CECs 2 (II), 3 (III) and 5 (V) passages post reconstitution of the virus as well as from 4 different tumor tissues (T1-T4) (upper panel). pRB-1B served as a a negative control (-) and pΔIR$_L$ as a positive control(+). Quality of all DNA samples was tested by a control PCR using the vIL-8 sequencing primer (lower panel).

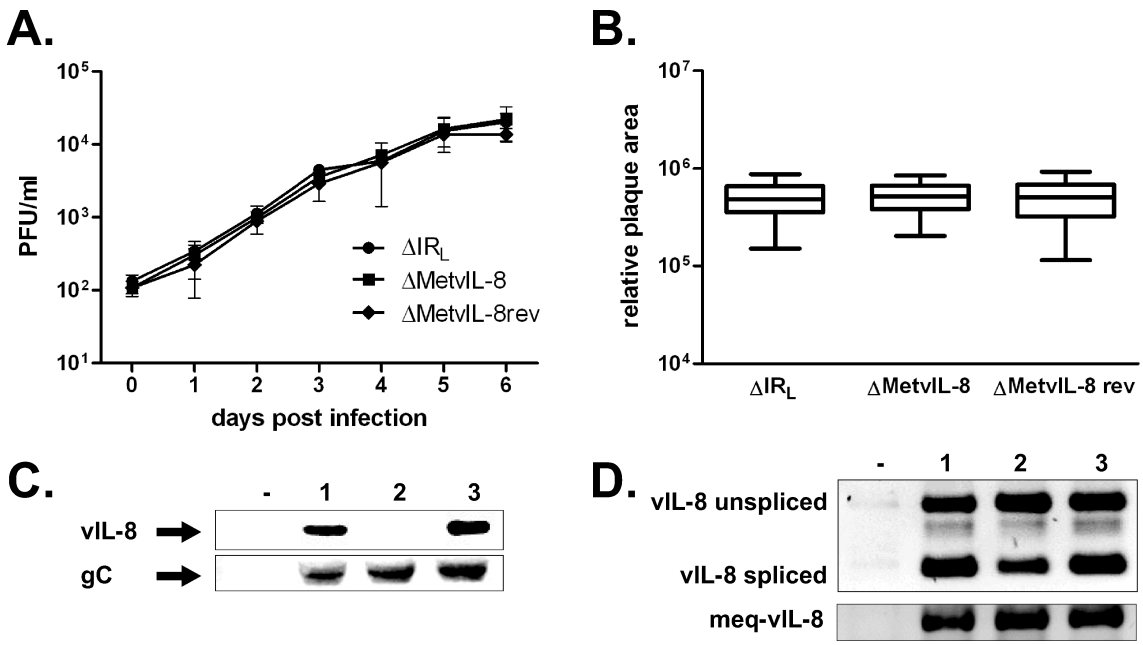

Figure 6: Mutation of the vIL-8 start codon abrogates vIL-8 expression but does not affect MDV replication or splicing in the region. A. Multiple step growth kinetics of vΔIR_L, vΔMet-vIL-8 and vΔMet-vIL-8rev shown as geometric mean with SEM. **B.** Plaque size assay of vΔIR_L, vΔMet-vIL-8 and vΔMet-vIL-8rev (n=135, One way ANOVA $p>0.05$). Plaque sizes are shown boxplots with minimum and maximum. **C.** Western blot analysis detecting vIL-8 (upper panel) or gC (lower panel) in the supernatant of CECs infected with indicated viruses. **D.** Analysis of vIL-8 (upper panel) and Meq-vIL-8 (lower panel) splicing by PCR in CECs infected vΔIR_L (1), vΔMet-vIL-8 (2) and vΔMet-vIL-8rev (3). Splice products described previously by Jarosinski and colleagues are detected.

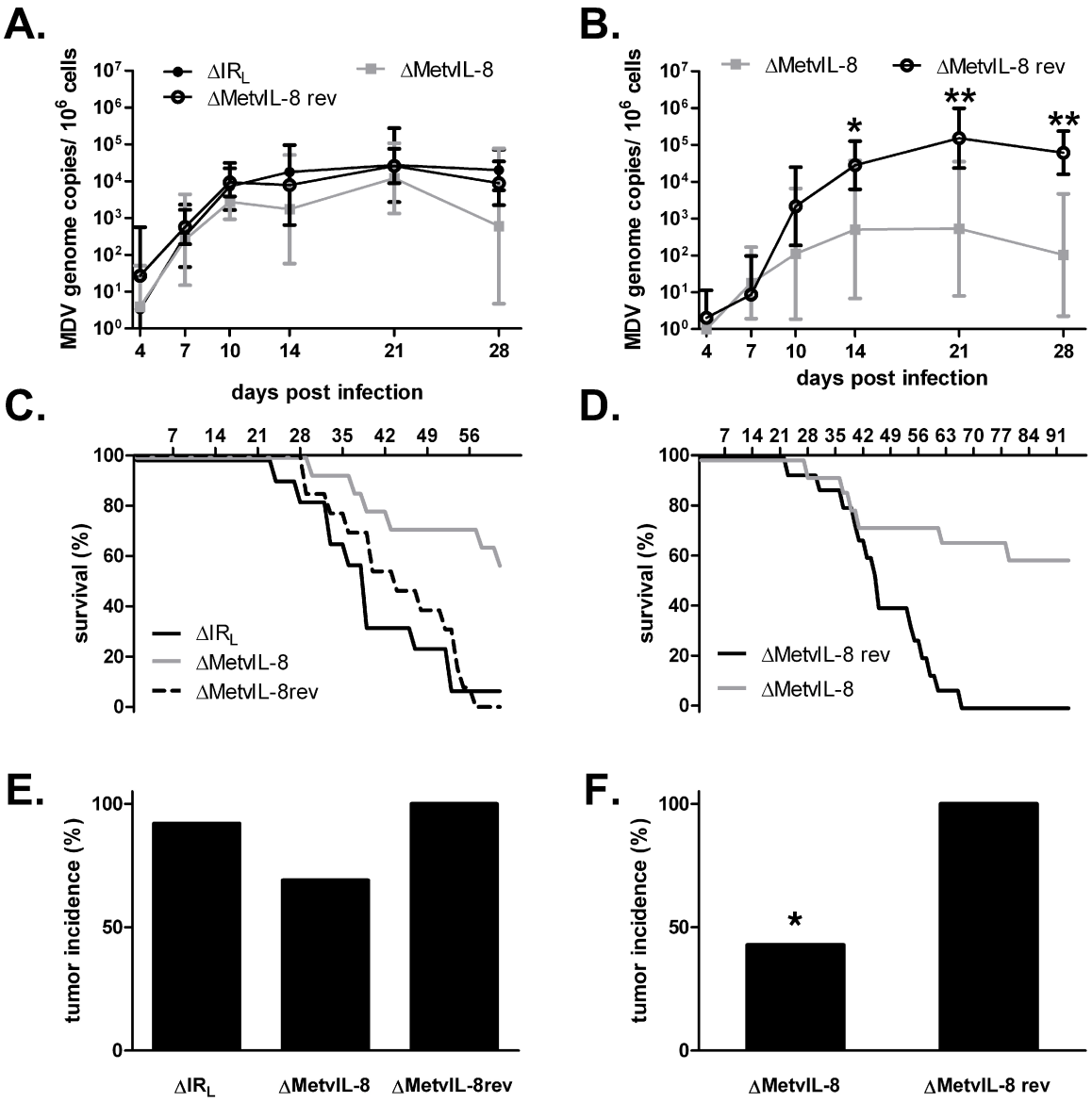

Figure 7: vIL-8 expression is dispensable for lytic replication but impairs disease development and tumor formation *in vivo*. A-B. qPCR analysis of the viral ICP4 gene and host iNOS gene. Blood samples of animals infected with ΔIR_L, vΔMetvIL-8 or vΔMetvIL-8 rev were taken at 4, 7, 10, 14, 21, and 28 dpi. Mean MDV genome copies per $1X10^6$ cells of eight infected chickens per group are shown. Viral titers in the blood in **A.** Exp-1(, Kruskal Wallis p>0,05 n=24 for all time points) and **B.** Exp-2 (Mann-Whitney-U, 14 dpi p=0,01, 21dpi and 28dpi p=0,002 n=24 for all time points) decreased in vΔMetvIL-8 infected animals when compared to vΔMetvIL-8 rev. **C-D.** Survival analysis of chickens infected with indicated viruses during **C.** Exp-1 and **D.** Exp-2. **E-F.** Tumor incidence in chickens infected with indicated viruses in **E.** Exp-1 (Fisher Freeman Hamilton, n=38 p>0.05) and **F.** Exp-2 (Fisher's exact, n=29 p<0.05). Necropsies were performed on chickens upon onset of clinical symptoms or after termination of the experiment. Tumor incidence is shown in percent of animals per group.

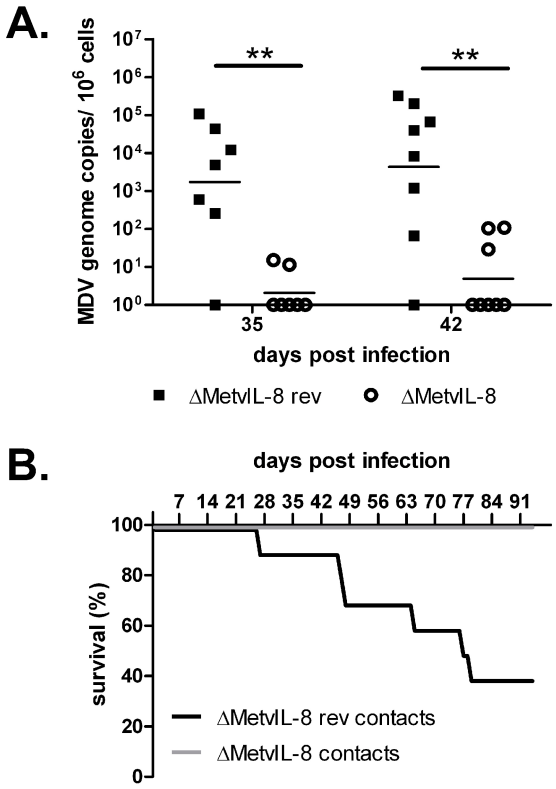

Figure 8. Disease and tumor development in animals infected with vΔMetvIL-8 via the natural route of infection. A. qPCR of MDV genome copies in the blood of chicken infected with indicated virus via the natural route of infection. Geometric means of MDV genome copies per $1X10^6$ cells are shown for 35 and 42 dpi (n=24, Mann-Whitney-U 35dpi and 42dpi p=0,007). **B.** Survival analysis of contact birds infected with indicated viruses

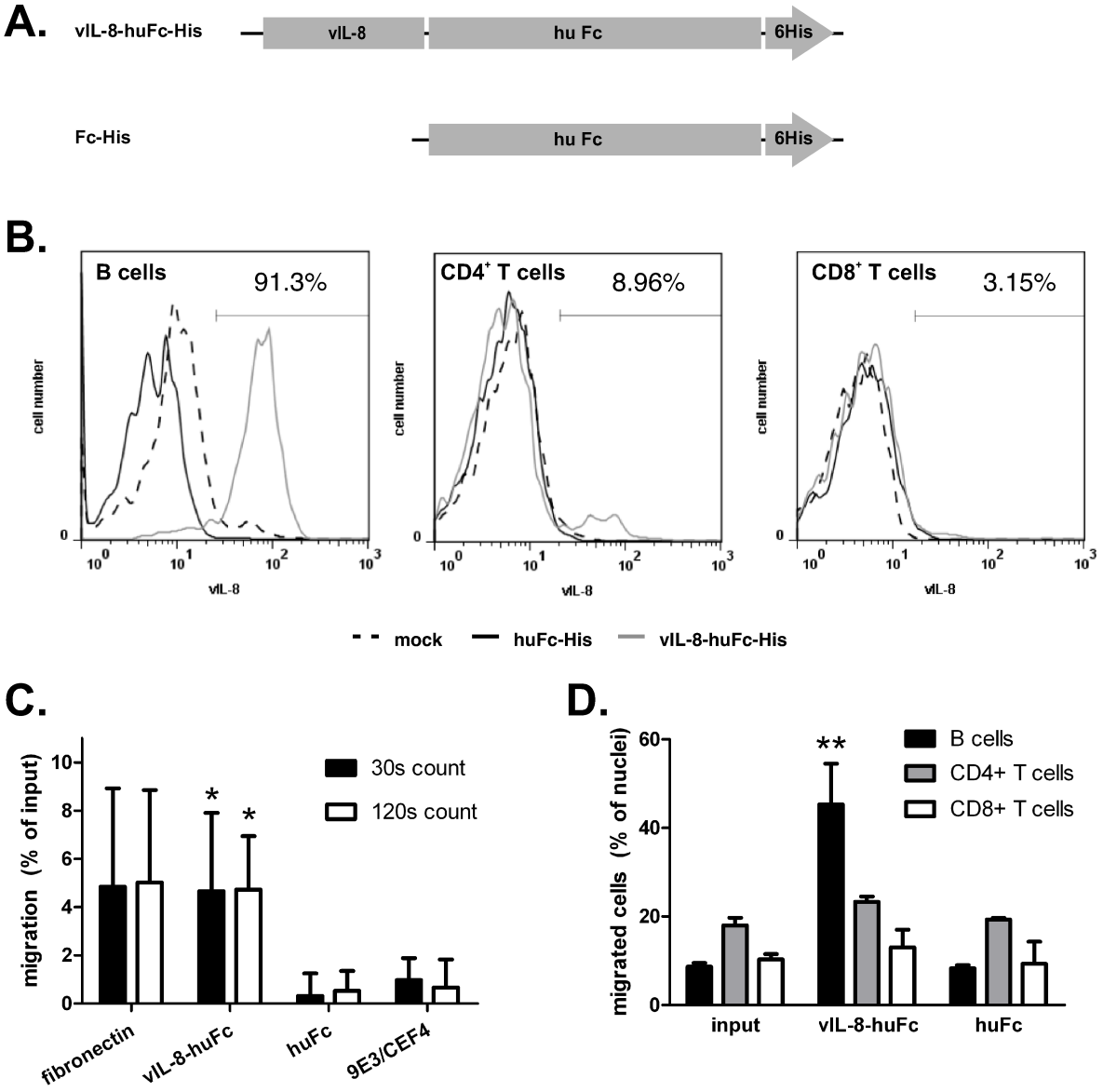

Figure 9. vIL-8 binds to and attracts B cells. **A.** Recombinant proteins used for binding and chemotaxis assay produced using the baculovirus expression system. **B.** Binding assay of recombinant vIL-8 to B cells (left panel), $CD4^+$ T cells (middle panel) or $CD8^+$ T cells (right panel). Data are shown as histograms and are representative for three independent experiments. Percentage of vIL-8 positive cells is indicated. **C.** Chemotaxis assay using vIL-8 as a chemoattractant for chicken blood PBMCs. Migrated cells were counted for the indicated time intervals by flow cytometry. Data are shown as percent of input cells normalized against background migration. Mean of 4 independent experiments (Bonferroni, 30s count n=12 p=0.042 (vIL-8 vs. Fc) and p=0.089 (vIL-8 vs. 9E3/CEF4); 120s count n=12 p=0.011 (vIL-8 vs. Fc) and p=0.013 (vIL-8 vs. 9E3/CEF4). **D.** Analysis of cell that migrated in chemotaxis assays. Data are presented as mean percentage of B cells, $CD4^+$ or $CD8^+$ T cells for each sample from three independent experiments (Bonferroni, B cells p=0.008, $CD4^+$ T cells p>0.05, $CD8^+$ T cells p>0.05 for vIL-8-huFc compared to either input or huFc).

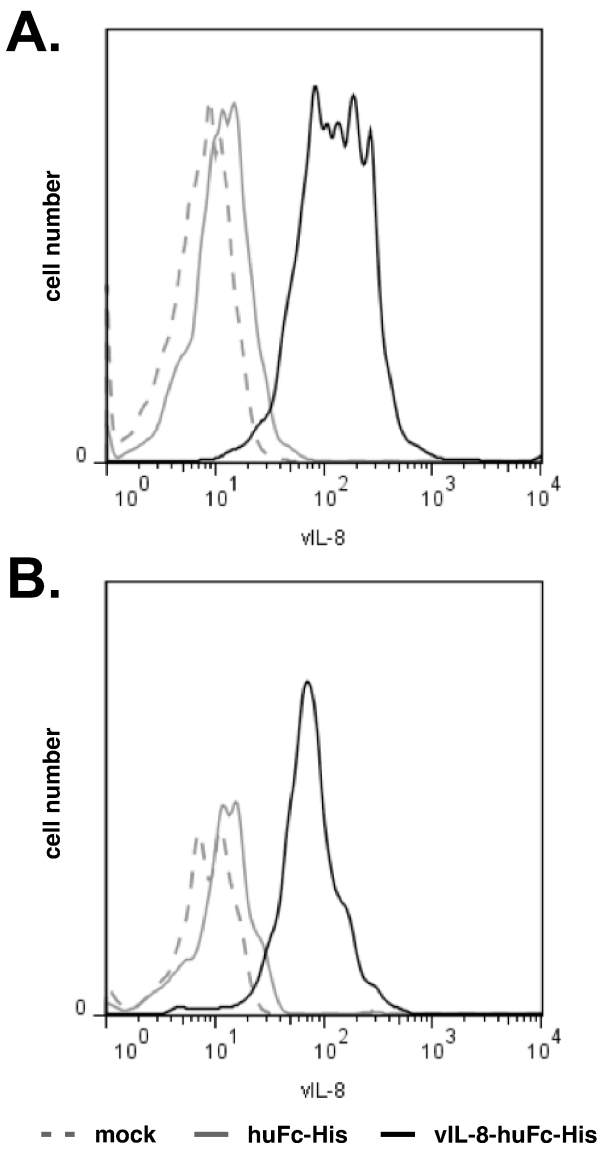

Figure 10. $CD25^+$ cells and $CD4^+CD25^+$ T cells bind vIL-8. A. Binding assay of recombinant vIL-8 to CD25 expressing cells. vIL-8 fluorescent intensity is shown for $CD25^+$ cells in the histogram. Data are representative for three independent experiments. **B.** Binding assay of recombinant vIL-8 to $CD4^+CD25^+$ T cells. vIL-8 fluorescent intensity is shown for $CD4^+CD25^+$ T cells in the histogram. Data are representative for three independent experiments.

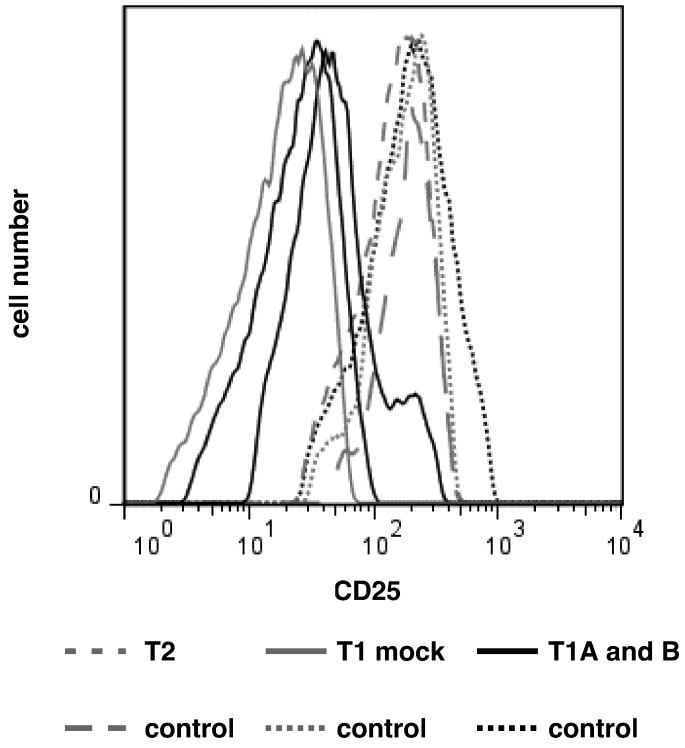

Figure 11: CD25 expression on vΔMetvIL-8 induced tumor cells. Tumor cells from chickens infected with vΔMetvIL-8, parental or revertant virus were stained for CD25. Fluorescent intensity for CD25 is shown in the histogram. Three tumor samples (T1A, T1B and T2) were analyzed from two different animals (T1 and T2). Mock control is exemplary shown for one tumor sample. Control tumors from wt infected animals are included.

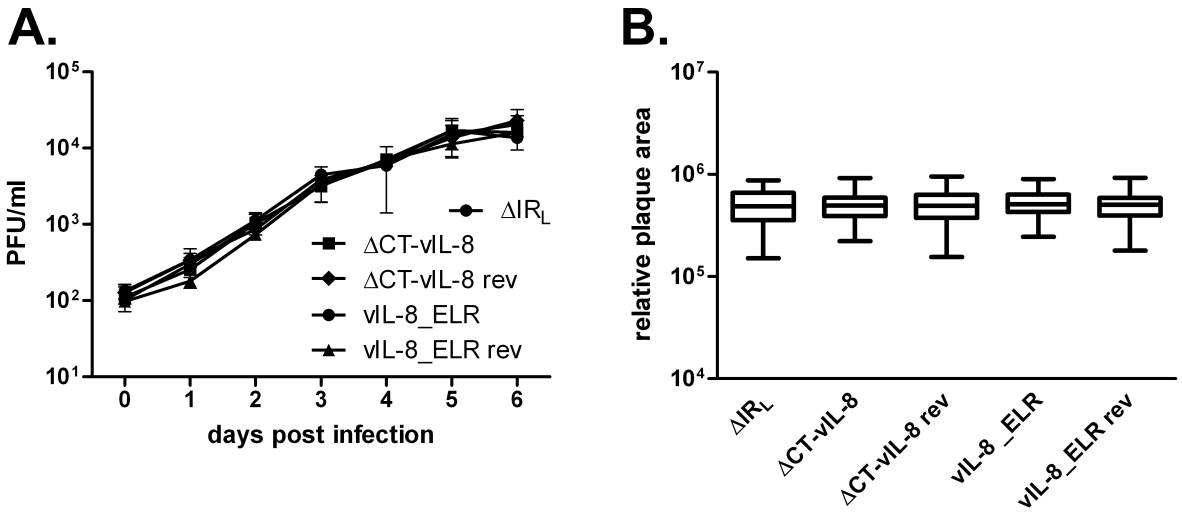

Figure 12: Replacement of the DKR motif by ELR in vIL-8 or deletion of the vIL-8 C-terminus does not influence viral replication *in vitro*. A. Multiple step growth kinetics of vΔIR$_L$, vΔCT-vIL-8, vΔCT-vIL-8 rev, vvIL-8_ELR and vvIL-8_ELR rev shown as geometric mean with SEM. **B.** Plaque size assay of vΔIR$_L$, vΔCT-vIL-8, vΔCT-vIL-8 rev, vvIL-8_ELR and vvIL-8_ELR rev (One way ANOVA $p>0.05$). Plaque sizes are shown as means with 95% confidence interval and SD.

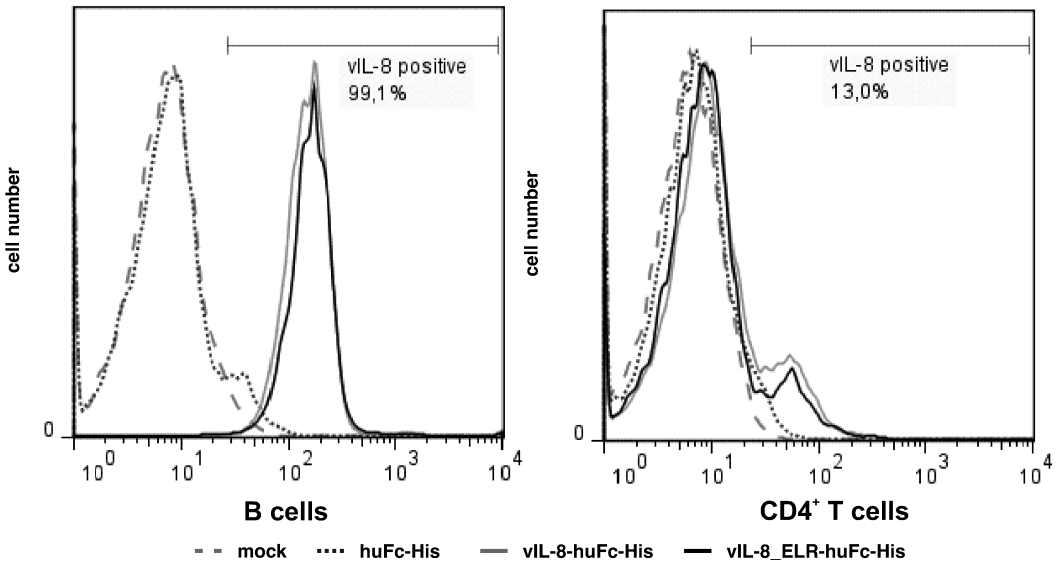

Figure 13: ELR has the same binding properties as vIl-8. Binding assay of recombinant vIL-8_ELR to B cells (left panel) and $CD4^+$ T cells (right panel). Data are shown as histograms and are representative for three independent experiments. Percentage of vIL-8 positive cells is indicated.

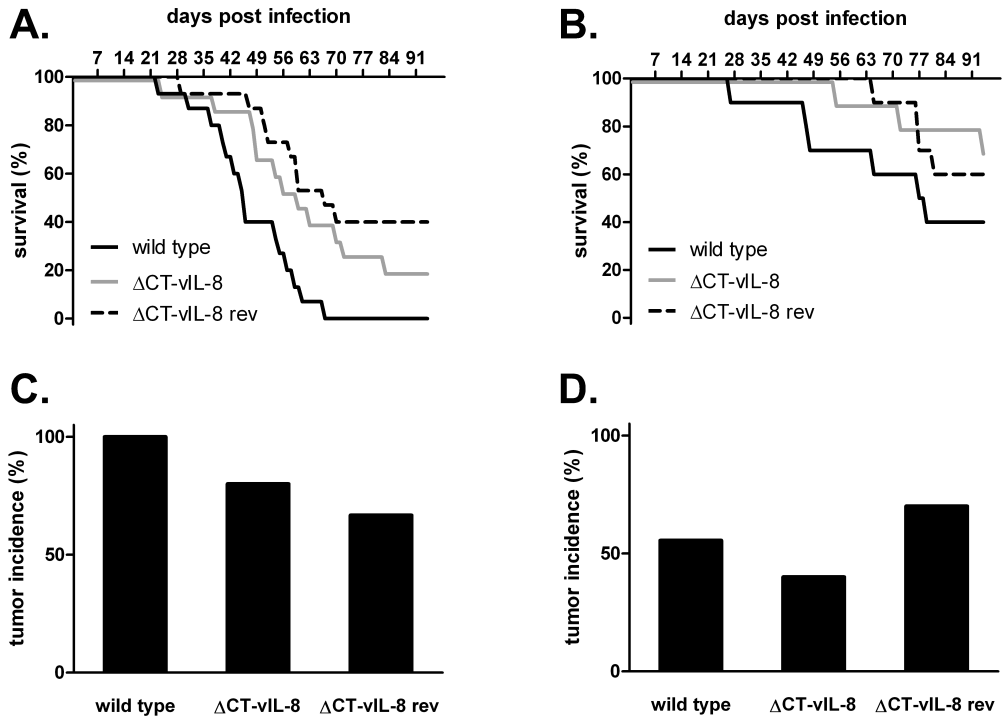

Figure 14: Deletion of vIL-8 C-terminus only has a minor impact on MD pathogenesis and tumor formation. A. Survival of chickens infected with vΔCT-vIL-8. MD incidence of 80% is only slightly reduced compared to MD incidence in RB-1B infected chickens which usually reaches 90-100%. **B.** Survival of chickens co-housed with vΔCT-vIL-8 infected chickens to study transmission. **C.** Tumor incidence upon termination of the experiment in vΔCT-vIL-8 infected chickens. **D.** Tumor incidence upon termination of the experiment in vΔCT-vIL-8 contact chickens. Fisher Freeman Hamilton ($p>0.05$).

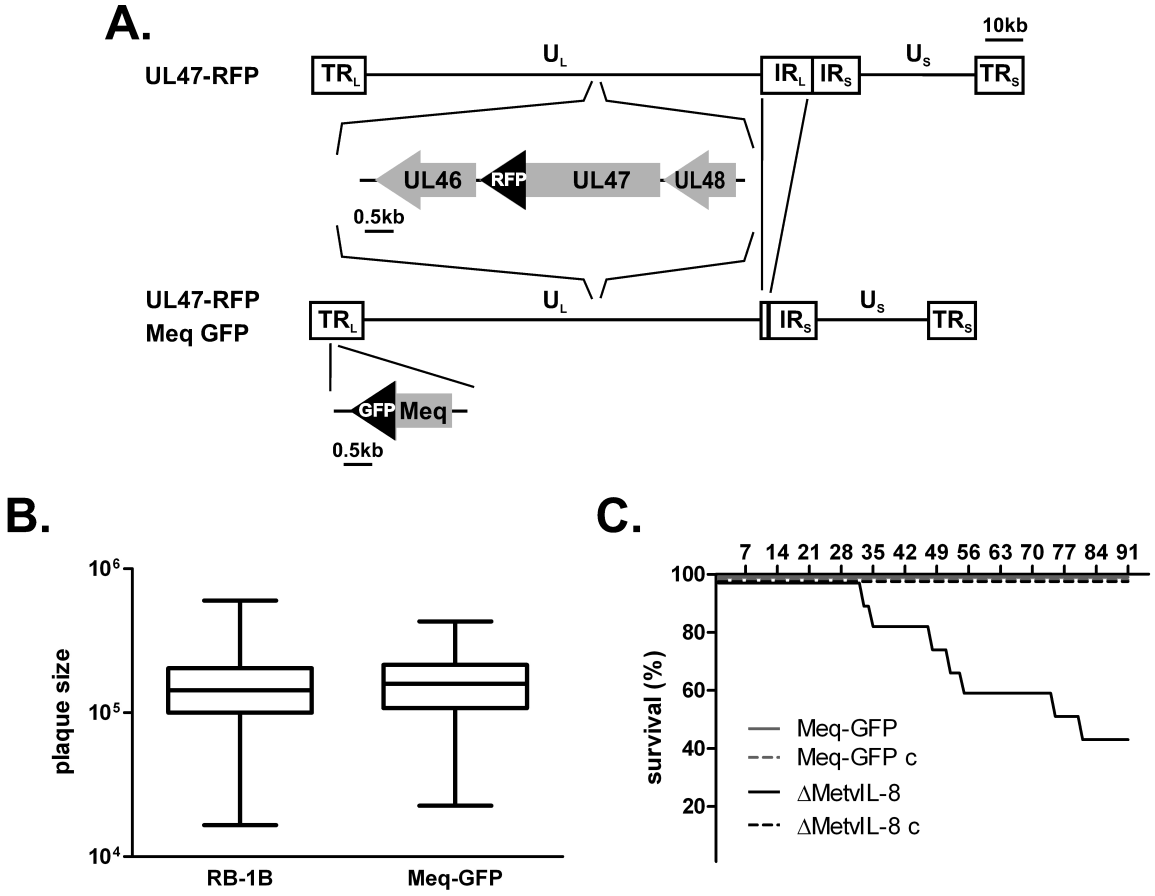

Figure 15: Characterization of vUL47-RFP_Meq-GFP*in vitro* and *in vivo*. A. Mutantions introduced into RB-1B-UL47RFP are shown. . **B**. Plaque size assay of vΔIR_L, vΔCT-vIL-8, vΔCT-vIL-8 rev, vvIL-8_ELR and vvIL-8_ELR rev (Mann-Whitney test, $p>0.05$). **C.** Survival of chickens infected with the markervirus vUL47-RFP_Meq-GFP or wild type virus. Another experiment run in parallel with vΔMetvIL-8 was as expected for infected and contact chickens and monitored until 91 dpi.

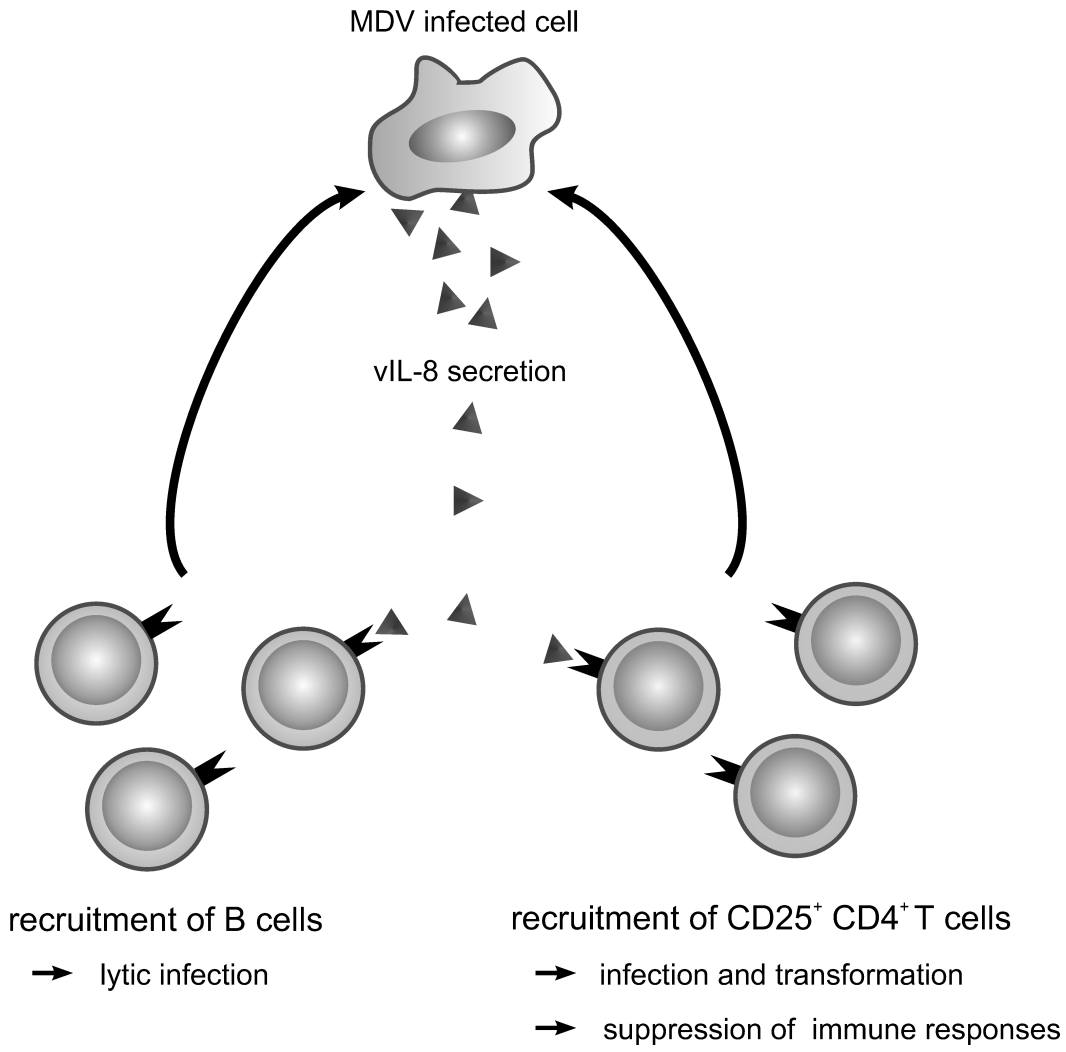

Figure 16. Model of vIL-8 functions during MD pathogenesis. vIL-8 is able to bind and recruit B cells to the site of infection leading to lytic infection of B cells that is necessary for efficient MDV replication in infected animals. Furthermore, vIL-8 can bind and attract $CD4^+CD25^+$ T cells that could serve as a target for MDV transformation. In addition, recruitment of $CD4^+CD25^+$ T_{reg} cells to tumor tissue could suppress immune responses at the site of infection.

References

Alcami, A. (2003). Viral mimicry of cytokines, chemokines and their receptors. *Nat Rev Immunol,* **3,** 36-50.

Alcami, A. and Koszinowski, U. H. (2000). Viral mechanisms of immune evasion. *Immunol Today,* **21,** 447-455.

Anobile, J. M., Arumugaswami, V., Downs, D., Czymmek, K., Parcells, M. and Schmidt, C. J. (2006). Nuclear localization and dynamic properties of the Marek's disease virus oncogene products Meq and Meq/vIL8. *J Virol,* **80,** 1160-1166.

Ansel, K. M., McHeyzer-Williams, L. J., Ngo, V. N., McHeyzer-Williams, M. G. and Cyster, J. G. (1999). In vivo-activated CD4 T cells upregulate CXC chemokine receptor 5 and reprogram their response to lymphoid chemokines. *J Exp Med,* **190,** 1123-1134.

Arvanitakis, L., Geras-Raaka, E., Varma, A., Gershengorn, M. C. and Cesarman, E. (1997). Human herpesvirus KSHV encodes a constitutively active G-protein-coupled receptor linked to cell proliferation. *Nature,* **385,** 347-350.

Ausländer, S. (2007). Aufreinigung und Charakterisierung monoklonaler Antikörper gegen Ochratoxin B. In: *Arbeitsgruppe für Human- und Umwelttoxikologie*, Vol. Bachelor of Science, Universität Konstanz, Konstanz, pp. 69.

Baaten, B. J., Staines, K. A., Smith, L. P., Skinner, H., Davison, T. F. and Butter, C. (2009). Early replication in pulmonary B cells after infection with Marek's disease herpesvirus by the respiratory route. *Viral Immunol,* **22,** 431-444.

Baigent, S. J., Davison, F. (2004). Marek's disease virus: biology and life cycle. In: *Marek's disease: an evolving problem*, P. Pastoret, Ed, Elsevier, pp. 62-77.

Baigent, S. J., Ross, L. J. and Davison, T. F. (1998). Differential susceptibility to Marek's disease is associated with differences in number, but not phenotype or location, of pp38+ lymphocytes. *J Gen Virol,* **79 (Pt 11),** 2795-2802.

Bataille, D. and Epstein, A. L. (1995). Herpes simplex virus type 1 replication and recombination. *Biochimie,* **77,** 787-795.

Biggs, P. M. (2004). Marek's disease - long and difficult beginnings. In: *Marek's disease: an evolving problem*, P. Pastoret, Ed, Elsevier, pp. 8-16.

Blackburn, E. H. (1991). Structure and function of telomeres. *Nature,* **350,** 569-573.

Boehmer, P. E. and Nimonkar, A. V. (2003). Herpes virus replication. *IUBMB Life,* **55,** 13-22.

Brazeau, E., Mahalingam, R., Gilden, D., Wellish, M., Kaufer, B. B., Osterrieder, N. and Pugazhenthi, S. (2010). Varicella-zoster virus-induced apoptosis in MeWo cells is accompanied by down-regulation of Bcl-2 expression. *J Neurovirol,* **16,** 133-140.

Bublot, M., Sharma J. (2004). Vaccination against Marek's disease. In: *Marek's disease: an evolving problem*, P. Pastoret, Ed, Elsevier, pp. 168-185.

Burgess, S. C. (2004). Marek's disease lymphomas. In: *Marek's disease: an evolving problem*, P. Pastoret, Ed, Elsevier, pp. 98-11.

Burgess, S. C. and Davison, T. F. (2002). Identification of the neoplastically transformed cells in Marek's disease herpesvirus-induced lymphomas: recognition by the monoclonal antibody AV37. *J Virol,* **76,** 7276-7292.

Burgess, S. C., Young, J. R., Baaten, B. J., Hunt, L., Ross, L. N., Parcells, M. S., Kumar, P. M., Tregaskes, C. A., Lee, L. F. and Davison, T. F. (2004). Marek's disease is a natural model for lymphomas overexpressing Hodgkin's disease antigen (CD30). *Proc Natl Acad Sci U S A,* **101,** 13879-13884.

Burnside, J., Bernberg, E., Anderson, A., Lu, C., Meyers, B. C., Green, P. J., Jain, N., Isaacs, G. and Morgan, R. W. (2006). Marek's disease virus encodes MicroRNAs that map to meq and the latency-associated transcript. *J Virol,* **80,** 8778-8786.

Calnek, B. W. (1986). Marek's disease--a model for herpesvirus oncology. *Crit Rev Microbiol,* **12,** 293-320.

Calnek, B. W. (2001). Pathogenesis of Marek's disease virus infection. *Curr Top Microbiol Immunol,* **255,** 25-55.

Calnek, B. W., Lucio, B., Schat, K. A. and Lillehoj, H. S. (1989). Pathogenesis of Marek's disease virus-induced local lesions. 1. Lesion characterization and cell line establishment. *Avian Dis,* **33,** 291-302.

Calnek, B. W., Schat, K. A., Ross, L. J., Shek, W. R. and Chen, C. L. (1984). Further characterization of Marek's disease virus-infected lymphocytes. I. In vivo infection. *Int J Cancer,* **33,** 389-398.

Calnek, B. W., Shek, W. R. and Schat, K. A. (1981). Spontaneous and induced herpesvirus genome expression in Marek's disease tumor cell lines. *Infect Immun,* **34,** 483-491.

Campadelli-Fiume, G., Amasio, M., Avitabile, E., Cerretani, A., Forghieri, C., Gianni, T. and Menotti, L. (2007). The multipartite system that mediates entry of herpes simplex virus into the cell. *Rev Med Virol,* **17,** 313-326.

Campbell, J. J. and Butcher, E. C. (2000). Chemokines in tissue-specific and microenvironment-specific lymphocyte homing. *Curr Opin Immunol,* **12,** 336-341.

Carrozza, J. H., Fredrickson, T. N., Prince, R. P. and Luginbuhl, R. E. (1973). Role of desquamated epithelial cells in transmission of Marek's disease. *Avian Dis,* **17,** 767-781.

Churchill, A. E. and Biggs, P. M. (1967). Agent of Marek's disease in tissue culture. *Nature,* **215,** 528-530.

Churchill, A. E., Chubb, R. C. and Baxendale, W. (1969). The attenuation, with loss of oncogenicity, of the herpes-type virus of Marek's disease (strain HPRS-16) on passage in cell culture. *J Gen Virol,* **4,** 557-564.

Cinamon, G., Grabovsky, V., Winter, E., Franitza, S., Feigelson, S., Shamri, R., Dwir, O. and Alon, R. (2001a). Novel chemokine functions in lymphocyte migration through vascular endothelium under shear flow. *J Leukoc Biol,* **69,** 860-866.

Cinamon, G., Shinder, V. and Alon, R. (2001b). Shear forces promote lymphocyte migration across vascular endothelium bearing apical chemokines. *Nat Immunol,* **2,** 515-522.

Clark-Lewis, I., Dewald, B., Geiser, T., Moser, B. and Baggiolini, M. (1993). Platelet factor 4 binds to interleukin 8 receptors and activates neutrophils when its N terminus is modified with Glu-Leu-Arg. *Proc Natl Acad Sci U S A,* **90,** 3574-3577.

Clark-Lewis, I., Schumacher, C., Baggiolini, M. and Moser, B. (1991). Structure-activity relationships of interleukin-8 determined using chemically synthesized analogs. Critical role of NH2-terminal residues and evidence for uncoupling of neutrophil chemotaxis, exocytosis, and receptor binding activities. *J Biol Chem,* **266,** 23128-23134.

Cui, X., Lee, L. F., Reed, W. M., Kung, H. J. and Reddy, S. M. (2004). Marek's disease virus-encoded vIL-8 gene is involved in early cytolytic infection but dispensable for establishment of latency. *J Virol,* **78,** 4753-4760.

Cyster, J. G., Ansel, K. M., Reif, K., Ekland, E. H., Hyman, P. L., Tang, H. L., Luther, S. A. and Ngo, V. N. (2000). Follicular stromal cells and lymphocyte homing to follicles. *Immunol Rev,* **176,** 181-193.

Davison, A. J., Dargan, D. J. and Stow, N. D. (2002). Fundamental and accessory systems in herpesviruses. *Antiviral Res,* **56,** 1-11.

Davison, F. and Nair, V. (2005). Use of Marek's disease vaccines: could they be driving the virus to increasing virulence? *Expert Rev Vaccines,* **4,** 77-88.

Delecluse, H. J. and Hammerschmidt, W. (1993). Status of Marek's disease virus in established lymphoma cell lines: herpesvirus integration is common. *J Virol,* **67,** 82-92.

Delecluse, H. J., Schuller, S. and Hammerschmidt, W. (1993). Latent Marek's disease virus can be activated from its chromosomally integrated state in herpesvirus-transformed lymphoma cells. *EMBO J,* **12,** 3277-3286.

Ellis, M. N., Eidson, C. S., Brown, J., Fletcher, O. J. and Kleven, S. H. (1981). Serological responses to Mycoplasma synoviae in chickens infected with virulent or avirulent strains of Marek's disease virus. *Poult Sci,* **60,** 1344-1347.

Fragnet, L., Blasco, M. A., Klapper, W. and Rasschaert, D. (2003). The RNA subunit of telomerase is encoded by Marek's disease virus. *J Virol,* **77,** 5985-5996.

Fragnet, L., Kut, E. and Rasschaert, D. (2005). Comparative functional study of the viral telomerase RNA based on natural mutations. *J Biol Chem,* **280,** 23502-23515.

Gimeno, I. (2004). Future strategies for controlling Marek's disease. In: *Marek's disease: an evolving problem*, P. Pastoret, Ed, Elsevier.

Guinamard, R., Signoret, N., Ishiai, M., Marsh, M., Kurosaki, T. and Ravetch, J. V. (1999). B cell antigen receptor engagement inhibits stromal cell-derived factor (SDF)-1alpha chemotaxis and promotes protein kinase C (PKC)-induced internalization of CXCR4. *J Exp Med,* **189,** 1461-1466.

Gunn, M. D., Ngo, V. N., Ansel, K. M., Ekland, E. H., Cyster, J. G. and Williams, L. T. (1998). A B-cell-homing chemokine made in lymphoid follicles activates Burkitt's lymphoma receptor-1. *Nature,* **391,** 799-803.

Hamroun, D., Desmet, F. and Lalande, M. (2010). Human Splicing Finder v. 2.4.1. http://www.umd.be/HSF/.

Hebert, C. A., Vitangcol, R. V. and Baker, J. B. (1991). Scanning mutagenesis of interleukin-8 identifies a cluster of residues required for receptor binding. *J Biol Chem,* **266,** 18989-18994.

Heldwein, E. E. and Krummenacher, C. (2008). Entry of herpesviruses into mammalian cells. *Cell Mol Life Sci,* **65,** 1653-1668.

Islam, A. F., Wong, C. W., Walkden-Brown, S. W., Colditz, I. G., Arzey, K. E. and Groves, P. J. (2002). Immunosuppressive effects of Marek's disease virus (MDV) and herpesvirus of turkeys (HVT) in broiler chickens and the protective effect of HVT vaccination against MDV challenge. *Avian Pathol,* **31,** 449-461.

Jarosinski, K. W., Arndt, S., Kaufer, B. B. and Osterrieder, N. (2012). Fluorescently tagged pUL47 of Marek's disease virus reveals differential tissue expression of the tegument protein in vivo. *J Virol,* **86,** 2428-2436.

Jarosinski, K. W., Margulis, N. G., Kamil, J. P., Spatz, S. J., Nair, V. K. and Osterrieder, N. (2007a). Horizontal transmission of Marek's disease virus requires US2, the UL13 protein kinase, and gC. *J Virol,* **81,** 10575-10587.

Jarosinski, K. W., Margulis, N. G., Kamil, J. P., Spatz, S. J., Nair, V. K. and Osterrieder, N. (2007b). Horizontal transmission of Marek's disease virus requires US2, the UL13 protein kinase, and gC. *J Virol,* **81,** 10575-10587.

Jarosinski, K. W., Osterrieder, N., Nair, V. K. and Schat, K. A. (2005). Attenuation of Marek's disease virus by deletion of open reading frame RLORF4 but not RLORF5a. *J Virol,* **79,** 11647-11659.

Jarosinski, K. W. and Schat, K. A. (2007). Multiple alternative splicing to exons II and III of viral interleukin-8 (vIL-8) in the Marek's disease virus genome: the importance of vIL-8 exon I. *Virus Genes,* **34,** 9-22.

Jarosinski, K. W., Tischer, B. K., Trapp, S. and Osterrieder, N. (2006). Marek's disease virus: lytic replication, oncogenesis and control. *Expert Rev Vaccines,* **5,** 761-772.

Johnson, E. A., Burke, C. N., Fredrickson, T. N. and DiCapua, R. A. (1975). Morphogenesis of marek's disease virus in feather follicle epithelium. *J Natl Cancer Inst,* **55,** 89-99.
Kaiser, P., Poh, T. Y., Rothwell, L., Avery, S., Balu, S., Pathania, U. S., Hughes, S., Goodchild, M., Morrell, S., Watson, M., Bumstead, N., Kaufman, J. and Young, J. R. (2005). A genomic analysis of chicken cytokines and chemokines. *J Interferon Cytokine Res,* **25,** 467-484.
Kaiser, P., Wu, Z., Rothwell, L., Fife, M., Gibson, M., Poh, T. Y., Shini, A., Bryden, W. and Shini, S. (2009). Prospects for understanding immune-endocrine interactions in the chicken. *Gen Comp Endocrinol,* **163,** 83-91.
Kaufer, B. B., Jarosinski, K. W. and Osterrieder, N. (2011). Herpesvirus telomeric repeats facilitate genomic integration into host telomeres and mobilization of viral DNA during reactivation. *J Exp Med,* **208,** 605-615.
Kaufer, B. B., Trapp, S., Jarosinski, K. W. and Osterrieder, N. (2010). Herpesvirus telomerase RNA(vTR)-dependent lymphoma formation does not require interaction of vTR with telomerase reverse transcriptase (TERT). *PLoS Pathog,* **6,** e1001073.
Kleven, S. H., Eidson, C. S., Anderson, D. P. and Fletcher, O. J. (1972). Decrease of antibody response to Mycoplasma synoviae in chickens infected with Marek's disease herpesvirus. *Am J Vet Res,* **33,** 2037-2042.
Levy, A. M., Gilad, O., Xia, L., Izumiya, Y., Choi, J., Tsalenko, A., Yakhini, Z., Witter, R., Lee, L., Cardona, C. J. and Kung, H. J. (2005). Marek's disease virus Meq transforms chicken cells via the v-Jun transcriptional cascade: a converging transforming pathway for avian oncoviruses. *Proc Natl Acad Sci U S A,* **102,** 14831-14836.
Liashkovich, I., Hafezi, W., Kuhn, J. M., Oberleithner, H. and Shahin, V. (2011). Nuclear delivery mechanism of herpes simplex virus type 1 genome. *J Mol Recognit,* **24,** 414-421.
Mackay, C. R. (2001). Chemokines: immunology's high impact factors. *Nat Immunol,* **2,** 95-101.
Maione, T. E., Gray, G. S., Petro, J., Hunt, A. J., Donner, A. L., Bauer, S. I., Carson, H. F. and Sharpe, R. J. (1990). Inhibition of angiogenesis by recombinant human platelet factor-4 and related peptides. *Science,* **247,** 77-79.
Marek, J. (1907). Multiple Nervenentzündung (Polyneuritis) bei Hühnern. *Deutsche Tierärztliche Wochenschrift,* **15,** 417-421.
Mettenleiter, T. C. (2002). Herpesvirus assembly and egress. *J Virol,* **76,** 1537-1547.
Mettenleiter, T. C. (2006). Intriguing interplay between viral proteins during herpesvirus assembly or: the herpesvirus assembly puzzle. *Vet Microbiol,* **113,** 163-169.
Mettenleiter, T. C., Klupp, B. G. and Granzow, H. (2006). Herpesvirus assembly: a tale of two membranes. *Curr Opin Microbiol,* **9,** 423-429.
Mettenleiter, T. C., Klupp, B. G. and Granzow, H. (2009). Herpesvirus assembly: an update. *Virus Res,* **143,** 222-234.
Morgan, R., Anderson, A., Bernberg, E., Kamboj, S., Huang, E., Lagasse, G., Isaacs, G., Parcells, M., Meyers, B. C., Green, P. J. and Burnside, J. (2008). Sequence conservation and differential expression of Marek's disease virus microRNAs. *J Virol,* **82,** 12213-12220.
Mukaida, N. and Baba, T. (2012). Chemokines in tumor development and progression. *Exp Cell Res,* **318,** 95-102.
Niikura, M., Witter, R. L., Jang, H. K., Ono, M., Mikami, T. and Silva, R. F. (1999). MDV glycoprotein D is expressed in the feather follicle epithelium of infected chickens. *Acta Virol,* **43,** 159-163.
Osterrieder, N. (1999). Sequence and initial characterization of the U(L)10 (glycoprotein M) and U(L)11 homologous genes of serotype 1 Marek's Disease Virus. *Arch Virol,* **144,** 1853-1863.

Osterrieder, N., Kamil, J. P., Schumacher, D., Tischer, B. K. and Trapp, S. (2006). Marek's disease virus: from miasma to model. *Nat Rev Microbiol,* **4,** 283-294.

Osterrieder, N., Vautherot, J-F. (2004). The genome content of Marek's disease like viruses. In: *Marek's disease: an evolving problem*, P. Pastoret, Ed, Elsevier, pp. 17-31.

Parcells, M. S., Lin, S. F., Dienglewicz, R. L., Majerciak, V., Robinson, D. R., Chen, H. C., Wu, Z., Dubyak, G. R., Brunovskis, P., Hunt, H. D., Lee, L. F. and Kung, H. J. (2001). Marek's disease virus (MDV) encodes an interleukin-8 homolog (vIL-8): characterization of the vIL-8 protein and a vIL-8 deletion mutant MDV. *J Virol,* **75,** 5159-5173.

Pastoret, P. (2004). Introduction. In: *Marek's Disease: An Evolving Problem*, P. Pastoret, Ed, Elsevier, pp. 1-7.

Pati, S., Cavrois, M., Guo, H. G., Foulke, J. S., Jr., Kim, J., Feldman, R. A. and Reitz, M. (2001). Activation of NF-kappaB by the human herpesvirus 8 chemokine receptor ORF74: evidence for a paracrine model of Kaposi's sarcoma pathogenesis. *J Virol,* **75,** 8660-8673.

Payne, L. (2004). Pathological responses to infection. In: *Marek's disease virus: an evolving problem*, P. Pastoret, Ed, Elsevier, pp. 78-97.

Pellet P.E., R. B. (2007). The Family Herpesviridae: A Brief Introduction. In: *Fields Virology 5th edition*, H. P. M. Knipe D.M, Ed, Vol. 2, Lippincott Williams & Wilkins.

Qian, Z., Brunovskis, P., Rauscher, F., 3rd, Lee, L. and Kung, H. J. (1995). Transactivation activity of Meq, a Marek's disease herpesvirus bZIP protein persistently expressed in latently infected transformed T cells. *J Virol,* **69,** 4037-4044.

Roizman, B. (1979). The structure and isomerization of herpes simplex virus genomes. *Cell,* **16,** 481-494.

Roizman, B., Knipe, D.M., Whitley, R.J. (2007). Herpes Simplex Viruses. In: *Fields Virology 5th Edition*, H. P. M. Knipe D.M, Ed, Vol. 2, Lippincott Williams & Wilkins, pp. 2501-2601.

Schat, K. A. (2004). Marek's disease immunosuppression. In: *Marek's disease: an evolving problem*, P. Pastoret, Ed, Elsevier, pp. 142-155.

Schat, K. A., Calnek, B. W. and Fabricant, J. (1981). Influence of the bursa of Fabricius on the pathogenesis of Marek's disease. *Infect Immun,* **31,** 199-207.

Schumacher, D., Tischer, B. K., Fuchs, W. and Osterrieder, N. (2000). Reconstitution of Marek's disease virus serotype 1 (MDV-1) from DNA cloned as a bacterial artificial chromosome and characterization of a glycoprotein B-negative MDV-1 mutant. *J Virol,* **74,** 11088-11098.

Schumacher, D., Tischer, B. K., Trapp, S. and Osterrieder, N. (2005). The protein encoded by the US3 orthologue of Marek's disease virus is required for efficient de-envelopment of perinuclear virions and involved in actin stress fiber breakdown. *J Virol,* **79,** 3987-3997.

Shack, L. A., Buza, J. J. and Burgess, S. C. (2008). The neoplastically transformed (CD30hi) Marek's disease lymphoma cell phenotype most closely resembles T-regulatory cells. *Cancer Immunol Immunother,* **57,** 1253-1262.

Shanmugasundaram, R. and Selvaraj, R. K. (2011). Regulatory T cell properties of chicken CD4+CD25+ cells. *J Immunol,* **186,** 1997-2002.

Sharpe, R. J., Byers, H. R., Scott, C. F., Bauer, S. I. and Maione, T. E. (1990). Growth inhibition of murine melanoma and human colon carcinoma by recombinant human platelet factor 4. *J Natl Cancer Inst,* **82,** 848-853.

Shek, W. R., Calnek, B. W., Schat, K. A. and Chen, C. H. (1983). Characterization of Marek's disease virus-infected lymphocytes: discrimination between cytolytically and latently infected cells. *J Natl Cancer Inst,* **70,** 485-491.

Spear, P. G. and Longnecker, R. (2003). Herpesvirus entry: an update. *J Virol,* **77,** 10179-10185.

Staeheli, P., Puehler, F., Schneider, K., Gobel, T. W. and Kaspers, B. (2001). Cytokines of birds: conserved functions--a largely different look. *J Interferon Cytokine Res,* **21,** 993-1010.

Strieter, R. M., Polverini, P. J., Arenberg, D. A., Walz, A., Opdenakker, G., Van Damme, J. and Kunkel, S. L. (1995). Role of C-X-C chemokines as regulators of angiogenesis in lung cancer. *J Leukoc Biol,* **57,** 752-762.

Tan, X., Brunovskis, P. and Velicer, L. F. (2001). Transcriptional analysis of Marek's disease virus glycoprotein D, I, and E genes: gD expression is undetectable in cell culture. *J Virol,* **75,** 2067-2075.

Tischer, B. K. and Kaufer, B. B. (2012). Viral bacterial artificial chromosomes: generation, mutagenesis, and removal of mini-F sequences. *J Biomed Biotechnol,* **2012,** 472537.

Tischer, B. K., von Einem, J., Kaufer, B. and Osterrieder, N. (2006a). Two-step red-mediated recombination for versatile high-efficiency markerless DNA manipulation in Escherichia coli. *Biotechniques,* **40,** 191-197.

Tischer, B. K., von Einem, J., Kaufer, B. and Osterrieder, N. (2006b). Two-step red-mediated recombination for versatile high-efficiency markerless DNA manipulation in Escherichia coli. *Biotechniques,* **40,** 191-197.

Tortorella, D., Gewurz, B. E., Furman, M. H., Schust, D. J. and Ploegh, H. L. (2000). Viral subversion of the immune system. *Annu Rev Immunol,* **18,** 861-926.

Trapp, S., Parcells, M. S., Kamil, J. P., Schumacher, D., Tischer, B. K., Kumar, P. M., Nair, V. K. and Osterrieder, N. (2006). A virus-encoded telomerase RNA promotes malignant T cell lymphomagenesis. *J Exp Med,* **203,** 1307-1317.

Van de Walle, G. R., May, M. L., Sukhumavasi, W., von Einem, J. and Osterrieder, N. (2007). Herpesvirus chemokine-binding glycoprotein G (gG) efficiently inhibits neutrophil chemotaxis in vitro and in vivo. *J Immunol,* **179,** 4161-4169.

Waugh, D. J. and Wilson, C. (2008). The interleukin-8 pathway in cancer. *Clin Cancer Res,* **14,** 6735-6741.

Zhao, Y., Yao, Y., Xu, H., Lambeth, L., Smith, L. P., Kgosana, L., Wang, X. and Nair, V. (2009). A Functional MicroRNA-155 Ortholog Encoded by the Oncogenic Marek's Disease Virus. *J Virol,* **83,** 489-492.

Danksagung

Mein Dank gilt Prof. Dr. Nikolaus Osterrieder und Prof. Dr. Benedikt Kaufer, die durch ihre fortwährende hervorragende wissenschaftliche Betreuung und die vielen Anregungen zum erfolgreichen Abschluss dieser Dissertation beigetragen haben. Außerdem möchte ich mich Prof. Dr. Bernd Kaspers für sein Engagement und die spannenden Diskussionen über das Thema dieser Arbeit ganz herzlich danken.

Meinen Kollegen, insbesondere dem „MDV Lab“ möchte ich für den Teamgeist, den Spaß im Laboralltag und die Unterstützung vor allem bei den tierexperimentellen Arbeiten danken.

Bedanken möchte ich mich auch für die finanzielle Unterstützung durch Stipendien der International Max Planck Reasearch School for Infectious Diseases and Immunity und des GRK 1121 für Host-Pathogen Interactions, ohne die meine Promotion nicht möglich gewesen wäre.

Für den Ausgleich zum Promotionsalltag möchte ich mich ganz herzlich bei der OG Rüdersdorf und der OG PSV Berlin bedanken, die es beim Training immer geschafft haben, mich auf andere Gedanken zu bringen.

Den wichtigsten Beitrag zu dieser Arbeit haben jedoch mein Mann Odilo, meine Eltern, mein Bruder und meine Freunde geleistet, die mich in allen Höhen und Tiefen mit Liebe und Freundschaft unterstütz haben. Sie waren die besten Zuhörer, haben mich motiviert und an mich geglaubt, dafür bin ich ihnen unendlich dankbar.

Selbstständigkeitserklärung

Hiermit bestätige ich, dass ich die vorliegende Arbeit selbständig angefertigt habe. Ich versichere, dass ich ausschließlich die angegebenen Quellen und Hilfen Anspruch genommen habe.

Berlin, den 18.09.2012

Annemarie Engel